DMD Fast Forward. Published on May 25, 2021 as DOI: 10.1124/dmd.120.000346
This article has not been copyedited and formatted. The final version may differ from this version.

# 3,3'-Diindolylmethane (BioResponse DIM®) Exhibits Significant Metabolism Following Oral Dosing in Humans

Monica L. Vermillion Maier[1,2], Lisbeth K. Siddens[1], Sandra L. Uesugi[2], Jaewoo Choi[2], Scott W. Leonard[2], Jamie M. Pennington[2], Susan C. Tilton[1], Jordan N. Smith[3], Emily Ho[2,4], H.H. Sherry Chow[5], Bach D. Nguyen[1], Siva K. Kolluri[1] and David E. Williams[1,2]

[1]Department of Environmental and Molecular Toxicology and the [2]Linus Pauling Institute, Oregon State University, Corvallis, OR, [3]Systems Toxicology & Exposure Science, Pacific Northwest National Laboratory, Richland, WA, [4]School of Biological and Population Health Sciences, Oregon State University, Corvallis, OR, [5]Cancer Center, University of Arizona, Tucson, AZ, United States

DMD Fast Forward. Published on May 25, 2021 as DOI: 10.1124/dmd.120.000346
This article has not been copyedited and formatted. The final version may differ from this version.

Running Title: 3,3'-Diindolylmethane Metabolites in Plasma and Urine

Corresponding Author: David E. Williams, Ph.D., Department of Environmental and Molecular Toxicology, Oregon State University, Corvallis, OR, 97331, USA, (PH) 1-541-737-3277, (FAX) 541 737-0497, david.williams@oregonstate.edu

Text Pages 22

Tables 2

Figures 8

Schemes 1

References 68

Abstract 250 words

Introduction 1,196 words

Discussion 1,708 words

Abbreviations: AHR, Aryl Hydrocarbon Receptor; AMS, accelerator mass spectrometry; AR, androgen receptor; BaP, benzo[*a*]pyrene; BR-DIM, BioResponse DIM® 150; CE, collision energy; CYP, Cytochrome P-450; DIM, 3,3'-diindolylmethane; DIM-O-glucuronide, 3-((1*H*-indole-3-yl)methyl)indolin-2-one-O-glucuronide and/or bis(1*H*-indol-3-yl)methanol-O-glucuronide; DIM-O-sulfate, 3-((1*H*-indole-3-yl)methyl)indolin-2-one-O-sulfate and/or bis(1*H*-indol-3-yl)methanol-O-sulfate; $E_2$, β-estradiol; ER, estrogen receptor; FDA-IND, Food and Drug Administration-Investigational New Drug; FICZ, 6-formylindolo[3,2-*b*]carbazole; GST, glutathione-*S*-transferase; I3C, indole-3-carbinol; ICZ, [3,2-*b*]indolocarbazole; IND, indole; mIND, 3-methylindole; 2-ox-mIND, 2-ox-3-methylindole; 3-methylenehydroxy-DIM, bis(1*H*-indol-3-yl)methanol; 3-methylenehydroxy-2-ox-DIM, 3-[hydroxy-(1*H*-indol-3-yl)-methyl]-1,3-dihydro-2-oxindole;

DMD Fast Forward. Published on May 25, 2021 as DOI: 10.1124/dmd.120.000346
This article has not been copyedited and formatted. The final version may differ from this version.

3-methylenehydroxy-DIM-O-sulfate, 3-((1*H*-indole-3-yl)methyl)indolin-2-one-O-sulfate and/or bis(1*H*-indol-3-yl)methanol-O-sulfate; 3-methylenehydroxy-2-ox-DIM-O-sulfate, 3-[hydroxy-(1*H*-indol-3-yl)-methyl]-1,3-dihydro-2-oxindole-O-sulfate; MPA, mobile phase A; MPB, mobile phase B; OATP, organic anion-transporting polypeptides; 2-ox-DIM, 3-((1*H*-indole-3-yl)methyl)indolin-2-one; pyrano-DIM, 5a,6a,11b-tetrahydro-5-H-pyrano[,2,3-b:6,5-b']diindole; SULT, sulfotransferase; UGT, UDP-glucuronosyltransferase

DMD Fast Forward. Published on May 25, 2021 as DOI: 10.1124/dmd.120.000346
This article has not been copyedited and formatted. The final version may differ from this version.

## Abstract

3,3'-Diindolylmethane (DIM), a major phytochemical derived from ingestion of cruciferous vegetables, is also a dietary supplement. In preclinical models, DIM is an effective cancer chemopreventive agent and has been studied in a number of clinical trials. Previous pharmacokinetic studies in preclinical and clinical models have not reported DIM metabolites in plasma or urine following oral dosing and the pharmacological actions of DIM on target tissues is assumed to be solely via the parent compound. Seven subjects (6 males and 1 female) ranging from 26-65 years of age, on a cruciferous vegetable-restricted diet prior to and during the study, took 2 BioResponse-DIM® 150 mg capsules (45.3 mg DIM/capsule) every evening for one week with a final dose the morning of the first blood draw. A complete time course was performed with plasma and urine collected over 48 hours and analyzed by UPLC-MS/MS. In addition to parent DIM, two mono-hydroxylated metabolites and 1 di-hydroxylated metabolite, along with their sulfate and glucuronide conjugates, were present in both plasma and urine. Results reported here are indicative of significant phase 1 and phase 2 metabolism and differ from previous pharmacokinetic studies in rodents and humans which reported only parent DIM present following oral administration. 2-Ox-DIM, identified as one of the mono-hydroxylated products, exhibited greater potency and efficacy as an AHR agonist when tested in an XRE-luciferase reporter assay using Hepa1 cells. In addition to competitive phytochemical-drug adverse reactions, additional metabolites may exhibit pharmacological activity highlighting the importance of further characterization of DIM metabolism in humans.

DMD Fast Forward. Published on May 25, 2021 as DOI: 10.1124/dmd.120.000346
This article has not been copyedited and formatted. The final version may differ from this version.

## Significance Statement

3,3'-Diindolylmethane (DIM), derived from indole-3-carbinol in cruciferous vegetables, is an effective cancer chemopreventive agent in pre-clinical models and a popular dietary supplement currently in clinical trials. Pharmacokinetic studies to date have found little or no metabolites of DIM in plasma or urine. In marked contrast, we demonstrate rapid appearance of mono- and di-hydroxylated metabolites in human plasma and urine as well as their sulfate and glucuronide conjugates. The 2-ox-DIM metabolite exhibited significant AHR agonist activity emphasizing the need for further characterization of the pharmacological properties of DIM metabolites.

DMD Fast Forward. Published on May 25, 2021 as DOI: 10.1124/dmd.120.000346
This article has not been copyedited and formatted. The final version may differ from this version.

## Introduction

Cruciferous vegetables are a rich source of phytochemicals, such as sulforaphane (SFN) and indole-3-carbinol (I3C), are effective cancer chemoprevention agents in preclinical models (Bradfield and Bjeldanes,1987a; Hayes et al., 2008; Higdon et al., 2007; Wattenberg and Loub, 1978). Currently, there are 65 ongoing or completed clinical trials involving cruciferous vegetables or I3C/3,3'-diindolylmethane (DIM) (www.ClinicalTrials.gov, accessed 06/26/20). Results in clinical trials and epidemiology studies with cruciferous vegetables have a mixed record of success typically exhibiting a moderate degree of protection from cancer (Ambrosone and Tang, 2009; Kim and Park, 2009; Maruthanila et al., 2014; Minich and Bland, 2007; van Poppel et al. 1999). The variation in previous study results may in part depend upon experimental design but are also likely a function of dose. For example, to achieve a DIM dose equivalent to two 150 mg capsules of BR-DIM®, each containing 45.3 mg of DIM, it would require consumption of 1 kg of freeze-dried Brussels sprout powder (approximately 10.7 kg of fresh Brussels sprouts) (Shorey et al., 2013).

I3C taken orally undergoes acid condensation reactions forming the dimer DIM as well as linear and cyclic trimers (Bjeldanes et al., 1991; Bradfield and Bjeldanes, 1987a). Little or no I3C is found in systemic circulation of rats or humans following oral dosing and thus the pharmacological effects of I3C are assumed to be due to one or more acid condensation products (Reed et al, 2006; Stresser et al., 1995b). Other than DIM, the pharmacology and toxicology of few acid condensation products have been described. DIM, the initial and major product (~30% of I3C dose) formed by acid condensation of

DMD Fast Forward. Published on May 25, 2021 as DOI: 10.1124/dmd.120.000346
This article has not been copyedited and formatted. The final version may differ from this version.

I3C, is not subject to further condensation reactions and is often reported as the only I3C-derived indole in plasma following oral dosing (Reed et al., 2006).

DIM has been employed in numerous animal models of cancer prevention as well as in human clinical trials with a major focus on breast and prostate cancer (Bradlow, 2008; Dalessandri et al., 2004; Donovan et al., 2018; Heath et al., 2010; Hwang et al., 2016; Li and Sarkar, 2015; Paltsev et al., 2016; Thomson et al., 2017; reviewed in Higdon et al., 2007). Among many pathways impacted by DIM are those mediated by the aryl hydrocarbon (AHR) and estrogen (ER) receptors (Higdon et al., 2007; Thomson et al., 2017). The $K_d$ (90 nM) of DIM for AHR is modest compared to other I3C condensation products such as 6-formylindolo[3,2-*b*]carbazole (FICZ) or [3,2-*b*]indolocarbazole (ICZ) (0.07 and 0.19 nM, respectively) but maximum concentrations achievable *in vivo* are typically in the low μM range (Bjeldanes et al., 1991; Faust et al., 2017; Rannug et al., 1987). Protection against estrogen-driven breast cancer is thought to be due in part to AHR induction of the CYP 1 family with resultant enhancement of the ratio of 2-hydroxy-β-estradiol ($E_2$) to 16α-hydroxy-$E_2$ (Auborn et al., 2003; Jellinck et al., 1993; Lord et al., 2002).

Cruciferous vegetable-derived indoles including I3C and DIM are described as “blocking agents” in preclinical models as greatest efficacy is seen when given prior to and/or during carcinogen exposure (Fujioka et al., 2016; Stresser et al., 1994a; 1994b; Takahashi et al., 1995). The proposed mechanism is thought to be AHR-dependent induction of both phase 1 (CYPs) and 2 (glutathione-*S*-transferases and UDP-glucuronosyltransferases) enzymes (Bradfield and Bjeldanes, 1987b; Lampe et al., 2000; Navarro et al., 2009; Peterson et al., 2009; Walters et al., 2004).

DMD Fast Forward. Published on May 25, 2021 as DOI: 10.1124/dmd.120.000346
This article has not been copyedited and formatted. The final version may differ from this version.

This research is part of a larger study using UPLC-accelerator mass spectrometry to examine [$^{14}$C]-benzo[a]pyrene (BaP) toxicokinetics following oral microdosing and the possible effects of dietary intake on kinetics (Madeen et al., 2019). One component of this study involved administration of DIM (BioResponse®, BR-DIM® 150) daily for 1 week prior to [$^{14}$C]-BaP dosing to assess the importance of the blocking mechanism in humans toward an important dietary carcinogen. We performed UPLC-MS/MS analysis of plasma and urine prior to supplementation (T: -7 days), the morning (overnight fast) of [$^{14}$C]-BaP micro-dosing (T: 0) and at subsequent timed intervals (plasma, 0.25, 0.50, 1.0, 1.5, 2.0, 3.0, 4.0, 8.0, 24 and 48 hours; urine 0-6, 6-12, 12-24 and 24-48 hours). In contrast to previously published studies (Anderton et al., 2004; Paltsev et al., 2013; Reed et al., 2006; 2008; Sepkovic et al., 2001) we found rapid and significant sulfate and glucuronide conjugates of DIM in plasma and urine characterized by a marked interindividual variability. These conjugates were derived from 3-methylenehydroxy-DIM (tentatively identified as the breakdown product pyrano-DIM) with lesser amounts of 2-ox-DIM and 3-methylenehydroxy-2-ox-DIM. These findings support a rapid and significant metabolism after oral administration of BR-DIM® 150.

DMD Fast Forward. Published on May 25, 2021 as DOI: 10.1124/dmd.120.000346
This article has not been copyedited and formatted. The final version may differ from this version.

## Materials and Methods

All chemicals and solvents were HPLC, LC-MS, or Optima grade. DIM (D9568) as well as deconjugating enzymes (all from *Helix pomatia*) sulfatase (S9751), β-glucuronidase (G7017 and β-glucuronidase/arylsulfatase (BGALA-RO) were purchased from Sigma Aldrich (St. Louis, MO). Surine (S-020) was purchased from Cerillium (Round Rock, TX). [$^2H_2$]-DIM was a gift from Stephen S. Hecht (University of Minnesota, Minneapolis, MN). BR-DIM® (BioResponse-DIM® 150), a commercially available formulation with clinically demonstrated enhanced bioavailability, was generously provided by Dr. Michael Zeligs of BioResponse, L.L.C. under a Material Transfer Agreement with Oregon State University. $^1H$ (400 MHz, Varian) spectrum was recorded in DMSO-$d_6$. $^1H$ NMR chemical shifts are reported in ppm (δ) relative to tetramethylsilane with the solvent resonance employed as the internal standard (DMSO-$d_6$, (δ = 2.50 ppm). Data are reported as follows: chemical shift, multiplicity (s = singlet, bs = broad singlet, d = doublet, t = triplet, m = multiplet), coupling constants (Hz) and integration.

Synthesis of (3-((1H-indol-3-yl)methyl)indolin-2-one) (2-ox-DIM)

The 2-ox-DIM was synthesized according to a modification of Pillaiyar et al., (2017). Indole-3-carbaldehyde (4 mmol) and 2-oxindole (4 mmol) were dissolved in ethanol (20 mL). Benzylamine (44 µL, 0.4 mmol) and acetic acid (23 µL, 0.4 mmol) were added and refluxed for 5 hours. The reaction was monitored by TLC (hexanes/ethyl acetate = 1:1). The resulting mixture was cooled to 0°C, sodium borohydride (0.76 g, 20 mmol) added in small portions over 5 minutes at 0°C, and the mixture stirred at room temperature overnight. The reaction was quenched with a saturated aqueous solution of ammonium chloride, extracted with ethyl acetate three times, washed with brine, and the ethyl

DMD Fast Forward. Published on May 25, 2021 as DOI: 10.1124/dmd.120.000346
This article has not been copyedited and formatted. The final version may differ from this version.

acetate layer dried over anhydrous sodium sulfate. The ethyl acetate was then evaporated under reduced pressure and the residue purified by flash column chromatography (silica gel, hexanes/ethyl acetate = 5/1 to 3/1) to give product (442 mg, 42%, 2-ox-DIM, $R_f$ = 0.39, hexanes/ethyl acetate = 1:1). $^1$H NMR (400 MHz, DMSO-$d_6$) δ 10.75 (bs, -N1-H, 1H), 10.26 (bs, -$N_2$-H, 1H), 7.53 (d, J = 7.95 Hz, $C_3$-H, 1H), 7.29 (d, J = 8.02 Hz, $C_4$-H, 1H), 7.11-7.00 (m, $C_5$-H, 2H), 6.98 (m,$C_6$-H, 2H), 6.92 (m, $C_7$-H, 1H), 6.82 (td, J = 7.52, 0.96 Hz, $C_8$-H, 1H), 6.72 (d, J = 7.74 Hz, $C_9$-H, 1H), 3.78 (dd, J = 7.52, 4.73 Hz, $C_{10}$-H, 1H), 3.41 (dd, J = 14.7, 7.52 Hz, $C_{11}$-H, 1H), 3.12 (dd, J = 14.7, 7.52 Hz, $C_{12}$-H, 1H) (Supplemental Figure 1). HRMS (TOF-MS/ESI): m/z calculated for $C_{17}H_{15}N_2O^+$ $[M+H]^+$, 263.1179; found, 263.1179.

Recruitment and Enrollment of Volunteers, Dietary Restrictions and Food Diary

All protocols and procedures including plans for recruitment and volunteer informed consent documents followed the Declaration of Helsinki and were approved by the Oregon State University Institutional Review Board (protocol #8789 under FDA IND #117175 and registered at ClinicalTrials.gov (identifier NCT03802721)). Healthy men and women ages 21-65 were recruited from the local community. Exclusion criteria included smoking of tobacco or other substances or use of smokeless tobacco in the past 3 months; a history of kidney, liver or gastrointestinal diseases such as Crohn's disease, ulcerative colitis, Celiac disease or gastrointestinal surgery; the use of medications that affect gut motility or nutrient absorption; and allergy to cruciferous vegetables. Additionally, female volunteers were required to be postmenopausal or surgically sterile. Seven individuals were screened for eligibility, and all were enrolled after a health history review and physical exam by the study physician. Volunteers

DMD Fast Forward. Published on May 25, 2021 as DOI: 10.1124/dmd.120.000346
This article has not been copyedited and formatted. The final version may differ from this version.

included six males and one female, ranged from ages 26-65 years in age, and BMI 22.4-37.4. The demographics of volunteers are given in Table 1.

Volunteers were asked to avoid cruciferous vegetables and condiments (see Supplemental Table 1) such as mustard, horseradish, and wasabi or any supplements containing I3C or DIM for two weeks prior to time 0 hour and through the 48-hour study cycle. All foods and non-water beverages were recorded in a food diary that spanned 3 days prior to and throughout the 48-hour study cycle. Volunteers also completed the Arizona Cruciferous Vegetable Food Frequency Questionnaire (ACVFFQ) to assess their usual intake of cruciferous vegetables and condiments in the previous three months (Thomson et al., 2016).

Dosing of Volunteers with BioResponse DIM® 150 and Collection of Blood and Urine

Volunteers were instructed to consume 2 capsules (300 mg total) of BioResponse DIM® 150 (45.3 mg DIM/capsule) each evening with dinner for 7 days prior to the 48-hour study cycle. Based on self-report capsule intake diaries, compliance was 100%. Volunteers also consumed 2 BR-DIM capsules at the start of the 48-hour pharmacokinetic study (T: 0).

Prior to consumption of BR-DIM capsules (T: -7 days), spot urine and 25 mL of blood were collected for baseline analysis. Subjects were instructed to fast overnight (10-12 hours) prior to the 48-hour study cycle. In the morning, prior to final DIM dosing, an indwelling catheter was placed in an antecubital vein and a spot urine and 25 mL of blood collected. Blood was sampled at 0, 0.25 0.5, 1.0, 1.5, 2, 3, 4, 8, 24, and 48 hours. Samples at 0-4 hours were collected from the catheter and 8-48 hour samples by

DMD Fast Forward. Published on May 25, 2021 as DOI: 10.1124/dmd.120.000346
This article has not been copyedited and formatted. The final version may differ from this version.

straight stick phlebotomy. Breakfast was provided after 2 hours. Volunteers were instructed to collect all urine from 0-48 hours in a separate amber glass container for each voiding. Urine was pooled for the 0-6, 6-12, 12-24, and 24-48 hour collections. To protect confidentiality, all specimens were deidentified at time of collection.

Extraction of Plasma and Urine for DIM and Metabolite Quantitation

Urine or plasma (1 mL) was adjusted to pH 5.0 with 0.06 M sulfuric acid. A mixture of β-glucuronidase (100,00 Fishman units/mL) and arylsulfatase (800,000 Roy units/mL) was added and incubated (37°C) overnight (18-20 hours). An internal standard, [$^{2}H_{2}$]-DIM was added and samples extracted with 4 mL methyl *tert*-butyl ether (plasma) or ethyl acetate (urine) (Staub et al., 2006). For extraction, samples were mixed by hand inversion for 1 min, centrifuged for 5 min at 2,000 x g, and aliquots evaporated to dryness under a gentle stream of nitrogen. Samples were reconstituted in 200 µL water:acetonitrile (90:10, v:v), centrifuged at 2,000 x g for 10 min, and transferred to low volume injection vials. Spiked synthetic urine (Surine) was used to prepare quality control samples. Samples were stored at -20°C until UPLC-MS/MS analysis.

UPLC-MS/MS Quantitation of DIM and Metabolites in Plasma and Urine

Quantitative analysis was performed on a Shimadzu (Shimadzu Scientific, Inc. Columbia, MD) Nexera LC-30AD UPLC system interfaced to a Shimadzu LCMS-8060 triple quadrupole mass spectrometer (MS/MS). The quantitation method was adapted from previously published methods (Baenas et al., 2017; Fujioka et al., 2014; Staub et al., 2006). Briefly, chromatographic separation was performed using a Waters (Milford, MA) ACQUITY UPLC BEH (2.1 x 50 mm, 1.7 µm) $C_{18}$ column with a gradient of water

DMD Fast Forward. Published on May 25, 2021 as DOI: 10.1124/dmd.120.000346
This article has not been copyedited and formatted. The final version may differ from this version.

(13 mM ammonium acetate, pH 4.0 with acetic acid; MPA) and acetonitrile (0.1% acetic acid; MPB). The gradient conditions were as follows: 10% MPB 0-0.2 min, linear increase to 60% MPB 0.2-5.0 min, 60% MPB 5.0-9.0 min, return to initial 9.0-9.1 min and hold 9.0-10.0 min at a flow rate of 0.18 mL/min. The column oven temperature was 40°C. Quantitation of DIM and 2-ox-DIM was determined daily by running a standard curve of instrument response versus injection (0-10 pmol) for the two standards.

Positive ion electrospray mass spectrometry and multiple reaction monitoring (MRM) was used for quantitative analysis. Compound-dependent parameters such as precursor/product ion information, voltage potentials (Q1 and Q3) and collision energy (CE) are shown in Supplemental Table 2. The dwell time was set at 20 msec. The optimal ESI conditions for detection of the analytes were: nebulizer gas, 2.9 L/min; heating gas, 10 L/min; drying gas, 10 L/min; interface temperature, 300°C; desolvation line temperature, 250°C; heat block temperature, 400°C. LabSolutions LCMS Ver.5.80 (Shimadzu Scientific, Inc. Columbia, MD) was used for data collection and quantitation.

Extraction of Non-Deconjugated Plasma and Urine for Structural Analysis

Plasma or urine (200 µL) was combined with cold 100% methanol (400 µL), mixed on a vortex for 30 sec, and incubated at -20°C 1 hr to precipitate proteins. Samples were centrifuged 10,000 x g 15 min at 4°C. Aliquots (525 µL) of supernatant were transferred to clean vials, evaporated to dryness with a nitrogen stream, and solubilized in 200 µL of 100% methanol. Samples were centrifuged at 2,000 x g for 5 min and transferred to low volume injection vials.

UPLC-MS/MS Analysis of DIM, Oxygenated DIM and Conjugates in Plasma and Urine

DMD Fast Forward. Published on May 25, 2021 as DOI: 10.1124/dmd.120.000346
This article has not been copyedited and formatted. The final version may differ from this version.

UPLC was performed with a Shimadzu Nexera system (Shimadzu; Columbia, MD) coupled to a high-resolution hybrid quadrupole-time-of-flight (TOF) mass spectrometer (MS) (TripleTOF® 5600; SCIEX; Framingham, MA). UPLC separations were as described above with a sample injection volume of 5 µL and flow rate of 0.18 mL/min. TOF-MS was operated with an acquisition time of 0.15 sec and a scan range of 60–1000 Da. MS/MS acquisition was performed with collision energy set at 40 V and collision energy spread of 15 V. Each MS/MS scan had an accumulation time of 0.1 sec and a range of 40–1000 Da using information-dependent acquisition (IDA). The source temperature was 500°C with IonSpray voltage at 5.5 kV in positive ion mode and -4.5 kV in negative ion mode, respectively. Data was processed using Peak View software Ver. 2.1 (SCIEX). Chromatographic peaks of metabolites were annotated using the extract ion chromatogram lists based on high accuracy MS, MS/MS fragmentation, and isotopic distribution.

Pharmacokinetic Analysis: Pharmacokinetics of DIM and metabolites were evaluated using non-compartmental and compartmental analyses. Area under the curve (AUC) of DIM and metabolite concentrations in plasma from time zero to the last measured time point and extrapolated to infinity (using last 3 time points) were calculated using the trapezoidal rule (Gibaldi and Perrier 1982). Mean residence times were calculated as a ratio of AUC under the 1$^{st}$ moment curve extrapolated to infinity to AUC extrapolated to infinity. Non-compartmental half-lives were calculated as the product of mean resident times with the natural log of two. A one-compartment pharmacokinetic model was used to evaluate the time course of DIM concentrations in plasma (Equations 1-3), where "*A0*", "*A1*", and "*A2*" represent the amount DIM in the absorption/formation and central

DMD Fast Forward. Published on May 25, 2021 as DOI: 10.1124/dmd.120.000346
This article has not been copyedited and formatted. The final version may differ from this version.

compartments, respectively; "*ka*", and "*ke*" are first-order rate constants. The concentration of the central compartment (C1) was calculated by normalizing the amount with the apparent volume of distribution (*V1*, L, Equation 3).

$$\frac{dA_0}{dt} = -(k_a \times A_0) \quad (1)$$

$$\frac{dA1}{dt} = (ka \times A0) - (ke \times A1) \quad (2)$$

$$C_1 = \frac{A_1}{V_1} \quad (3)$$

Optimizations of model parameters were obtained using a maximum log likelihood objective and the Nelder-Mead algorithm. Initial values were set by adjusting parameters visually. Software used to statistically analyze data was "R: A language and environment for statistical computing" Version 4.0.3 (R Foundation for Statistical Computing, Vienna, Austria).

AHR Reporter Assay: Hepa1 mouse hepatoma cells, transfected with a xenobiotic response element (XRE)-luciferase reporter were plated in 96 well plates at 1 x $10^4$ cells per well. After growth overnight, each well was treated with 0.1, 1.0 or 50 µM DIM or 2-ox-DIM (each concentration in triplicate in 0.1% DMSO) and incubated for 18-24 hours. Cells were lysed in 100 µL passive cell lysis reagent (Promega Corp., Madison, WI) for 15 minutes and luciferase activity measured using a luminometer (Tropix TR717 microplate luminometer, Applied Biosystem, Bedford, MA). The potent AHR indole ligand FICZ was used as a positive control at 0.1 µM.

DMD Fast Forward. Published on May 25, 2021 as DOI: 10.1124/dmd.120.000346
This article has not been copyedited and formatted. The final version may differ from this version.

## Results

Metabolites in Plasma

No DIM or DIM metabolites were detected prior to initiation of the one week of supplementation (T: -7 hr). After an overnight fast (10-12 hours after last daily DIM dose), urine and plasma were collected (T: 0 hr) and subjects given a final dose of DIM along with 50 ng of [$^{14}$C]-BaP. When plasma samples were treated with β-glucuronidase/sulfatase followed by extraction and UPLC-MS/MS, both $^{2}H_2$-DIM (249.10>132.05) and DIM (247.10>130.05) eluted at 7.00 minutes whereas the major polar metabolite (5.85 minutes), initially thought to be 2-ox-DIM (263.12>130.15), on closer examination eluted slightly later than the 2-ox-DIM standard (5.65 minutes) (Figure 1). Standard curves of instrument response versus pmol of DIM and 2-ox-DIM standards established that the latter generated a 70-fold greater signal (Figure 1). Utilizing the Sciex 5600 QTOF, 2-ox-DIM in the samples was confirmed by mass (< 5 ppm error), retention time, MS/MS fragmentation and isotope distribution. The major peak was tentatively identified as pyrano-DIM, formed spontaneously from 3-methylenehydroxy-DIM based on fragmentation pattern (Figure 2). Estimation of pyrano-DIM (3-methylenehydroxy-DIM) was done with the assumption that the instrument response was approximately equivalent to 2-ox-DIM. In addition to the two mono-hydroxylated metabolites, a significant amount of the di-hydroxylated metabolite, 3-methylenehydroxy-2-ox-DIM (279.09 > 146.06) was detected following deconjugation (Supplemental Figure 2). The identity of this metabolite was confirmed by mass accuracy (m/z 279.1128, MS/MS fragmentation (m/z 146.0592) and isotope distribution. This metabolite was not quantified owing to the lack of a di-hydroxylated standard. Our

DMD Fast Forward. Published on May 25, 2021 as DOI: 10.1124/dmd.120.000346
This article has not been copyedited and formatted. The final version may differ from this version.

TOF-MS/MS results are not consistent with hydroxylation of the phenyl ring in agreement with metabolism of DIM *in vitro* by MCF-7 cells.

The time course for appearance of DIM, 2-ox-DIM and pyrano-DIM in plasma treated with deconjugation enzymes is shown in Figure 3 for each of the seven subjects. A large interindividual variability is apparent with two individuals exhibiting little or no parent plasma DIM with robust yield of the pyrano-DIM. Pharmacokinetic analysis of the data was performed with both one- and non-compartmental models (Table 2). The mean $T_{max}$ values for DIM and pyrano-DIM and conjugates are 2.67 ± 0.98 and 2.96 ± 2.44 hours, respectively (Table 2A). The mean $C_{max}$ for DIM and the mono-hydroxylated metabolites and their respective conjugates, are 423 ± 610 and 1910 ± 3190 pmol/mL plasma, respectively (Table 2A). The $T_{max}$ and $C_{max}$ (average ~ 0.4 μM) for DIM is consistent with previous studies (Paltsev et al., 2013; Reed et al., 2008). Mean non-compartmental half-life, apparent clearance and apparent volume of distribution for DIM were 4.29 ± 2.48 hours, 161 ± 132 L x $hr^{-1}$ and 1010 ± 693 L, respectively. The relatively large apparent volume of distribution would indicate that little of the administered dose was in the central plasma compartment suggesting DIM was poorly absorbed or extensively distributed to other compartments. For comparison, non-compartmental half-lives for mono-hydroxylated metabolites and their conjugates was 9.34 ± 3.13.

A one-compartment model was utilized to estimate rate constants, apparent volume of distribution and half-life for DIM (Table 2B). The compartmental modeling approach estimated lower apparent volumes of distribution compared to the non-compartmental modeling approach (492 vs. 1010 L, respectively); however, they were still relatively high compared to body weights of volunteers suggesting low fraction of absorption

DMD Fast Forward. Published on May 25, 2021 as DOI: 10.1124/dmd.120.000346
This article has not been copyedited and formatted. The final version may differ from this version.

and/or high distribution to tissues. Again, the large standard deviation of the means for these pharmacokinetic constants reflect a large interindividual variability.

The metabolic profile was also analyzed for plasma not treated with deconjugation enzymes. The time course for appearance in plasma of the sulfate and glucuronide conjugates of mono-hydroxylated and di-hydroxylated DIM is shown in Figure 4. It is apparent that a significant amount of the DIM dose is present in plasma as sulfate and glucuronide conjugates of mono- (and di-) hydroxylated metabolites (Figure 4) throughout the time course, and 24 hours is sufficient to mostly clear the DIM dose from blood. DIM-O-sulfate and DIM-O-glucuronide represent conjugation at the 3-methylenehydroxy- and/or 2-ox-position. Although we cannot make a definitive assignment by TOF-MS/MS, based on the relative amounts of 2-ox-DIM and pyrano-DIM following deconjugation we can assume the large majority of conjugation occurred at the 3-methylenehydroxy position (Figure 3). The plasma levels at T: 0 for each metabolite includes the contribution from the previous night's DIM dose (little or no parent DIM present at T: 0). The $T_{max}$ for the conjugated metabolites is 2-3 hours similar to parent DIM. If one assumes a comparable instrument response, it appears that sulfate conjugates predominate.

Urinary Metabolites

Urine was collected 10-12 hours after the last of the 7 daily DIM doses (T: 0) and examined for DIM and DIM metabolites. As in plasma, upon deconjugation, pyrano-DIM was predominant (Figure 5) with much smaller amounts of 2-ox-DIM. Of the identified components in urine, parent DIM (29%) and 3-methylenehydroxy-DIM conjugates (70%) made up almost the entire profile (Figure 5). The relatively large apparent

DMD Fast Forward. Published on May 25, 2021 as DOI: 10.1124/dmd.120.000346
This article has not been copyedited and formatted. The final version may differ from this version.

volume of distribution would indicate that little of the orally administered dose was in the plasma compartment, which could suggest low oral absorption of DIM. In urine, we accounted for 5% of the administered DIM dose in urinary elimination of DIM, pyrano-DIM, and 2-ox-DIM. With respect to the time-course, DIM, 2-ox-DIM and pyrano-DIM in deconjugated samples from urine were observed at T: 0 (10-12 hours after the last of the daily doses) and peaked in the 6-12 hour pool. As in plasma, levels of pyrano-DIM were 2-3-fold higher than parent DIM.

In urine samples not treated with deconjugation enzymes there were abundant amounts of sulfate (Figure 6) and glucuronide (Figure 7) conjugation metabolites of 3-methylenehydroxy-DIM and 3-methylenehydroxy-2-ox-DIM. The morning following the last dose, urine was collected prior (T: 0 hr) to the final acute dose and pooled over the time periods 0-6, 6-12, 12-24 and 24-48 hours. With DIM supplementation there were still significant amounts of parent DIM, conjugated mono-hydroxylated metabolites and the di-hydroxylated metabolite, after the 10-12 hour fast just prior to the acute dose at T: 0 hours. The levels of metabolites decreased with time although there were still small amounts present in the 24-48 hour fraction. Urine collected from the seven volunteers just prior to initiation of DIM supplementation (T: -7 days) did not indicate the presence of DIM or any DIM metabolites (Figure 5) confirming the effectiveness of the implemented dietary restriction.

We compared non-compartmental half-lives of DIM and DIM metabolites in plasma and urine using a compartmental model. DIM metabolite half-lives in plasma and urine demonstrated good agreement (12.4 and 11.2 hours, respectively for 2-ox-DIM and for 3-methylenehydroxy-(pyrano)-DIM) 9.3 and 9.8 hours respectively, suggesting urine is

DMD Fast Forward. Published on May 25, 2021 as DOI: 10.1124/dmd.120.000346
This article has not been copyedited and formatted. The final version may differ from this version.

the primary route of elimination for the mono-hydroxylated metabolites (data not shown). In contrast, plasma and urine half-lives for DIM differed by 2-fold (4.3 and 8.6 hours, respectively), suggesting other processes, like metabolism, were at least partially responsible for clearing DIM. In this study, we measured urinary elimination of DIM, 3-methylenehydroxy-(pyrano)-DIM and 2-ox-DIM and their conjugates (Table 2) but have not accounted for potential routes of elimination such as feces or additional metabolites such as 3-methylenehydroxy-2-ox-DIM and all conjugates.

We tested the only metabolite standard available to us, 2-ox-DIM, in a mouse Hepa1 AHR reporter assay and found significantly greater efficacy with the metabolite, significant at 1 ($p=0.017$) and 50 ($p=0.031$) μM (Figure 8).

DMD Fast Forward. Published on May 25, 2021 as DOI: 10.1124/dmd.120.000346
This article has not been copyedited and formatted. The final version may differ from this version.

## Discussion

I3C is formed from hydrolysis of glucobrassicin by the plant and bacterial enzyme myrosinase. DIM is the major (~30%) condensation product formed from I3C in the stomach after oral ingestion and is considered the major bioactive indole from cruciferous vegetables, the dietary source of glucobrassicin. In fact, urinary levels of DIM have been shown to be an accurate biomarker of human dietary crucifer ingestion (Fujioka et al., 2016). DIM and I3C are popular dietary supplements and effective cancer chemopreventive agents in pre-clinical models. Clinical trials show promise especially with respect to ER-responsive breast cancer and androgen receptor (AR)-dependent prostate cancer (Heath et al., 2010; Hwang et al., 2016; Li and Sarkar, 2015; Thomson et al., 2016). I3C and DIM are also effective in treatment of cervical intraepithelial neoplasia (Ashrafian et al., 2015).

There are numerous mechanisms proposed for DIM's cancer chemoprevention including AHR-dependent induction of CYP1A2 with resultant increases in the ratio of 2-hydroxy- to 16α-hydroxy-E2 (Auborn et al., 2003; Jellinck et al., 1993; Lord et al., 2002). DIM can also modulate ER and AR signaling. important in prevention of breast and prostate cancers (Hwang et al., 2016; Marconett et al., 2010; Thomson et al., 2017). Other targets include components of cell cycle control and apoptosis (Aggarwal and Ichikawa, 2005; Bonnesen et al., 2001; Firestone and Bjeldanes, 2003; Hsu et al., 2008; Kim and Milner, 2005; Rajoria et al., 2011; Weng et al., 2008).

The AHR-dependent induction of CYPs 1A1, 1A2 and 1B1 alter the toxicokinetics of BaP in rodent models but at BaP doses orders of magnitude higher than daily human exposure. To examine the potential for DIM supplementation in alteration of the

DMD Fast Forward. Published on May 25, 2021 as DOI: 10.1124/dmd.120.000346
This article has not been copyedited and formatted. The final version may differ from this version.

toxicokinetics of oral BaP (>95% exposure is dietary) in humans at relevant environmental exposures we have utilized UPLC-accelerator mass spectrometry at Lawrence Livermore National Laboratory in an NIH-funded study with an FDA IND approval (Madeen et al., 2019). The study reported here was not designed as a DIM pharmacokinetic study although it resembles a previous protocol with I3C (Reed et al., 2006) in which women in a Phase 1 trial were given 200 mg I3C for 4 weeks followed by 4 weeks of 400 mg daily I3C. The pharmacokinetic study was then performed following an acute 400 mg dose after an overnight fast. Subsequent analysis of plasma only quantified DIM (no acid condensation products of I3C or DIM metabolites were detected). In a subsequent study Reed et al., (2008) found the $C_{max}$ for an acute dose of 200 mg DIM (104 ± 94 ng/mL) was similar (93 ± 30 ng/mL) to 600 mg I3C (Reed et al., 2006), although there was significant inter-individual variation and a small (n=3 plus 1 placebo for each of 6 different dose groups) sample size. Again, no DIM metabolites were reported. The inter-individual variation across the six dosage groups was not related to sex, age or BMI (Reed et al., 2008). Heath et al., (2010) also found high inter-individual variation (n=12 total men divided into 4 dose groups) in a phase 1 dose-escalation study of castrate-resistant, non-metastatic prostate cancer. In the present study we report a similar plasma $C_{max}$ (111 ± 160 ng/mL, n=7) for parent DIM in individuals dosed with 2 x 150 mg BR-DIM® 150 capsules each containing 45.3 mg DIM.

In this study upon examination of plasma and urine levels following an acute dose of DIM, 10-12 hours subsequent to 1 week of supplementation (2 x 150 mg BioResponse-DIM® 150 in the evening with dinner), we were struck by the amount of sulfate and

DMD Fast Forward. Published on May 25, 2021 as DOI: 10.1124/dmd.120.000346
This article has not been copyedited and formatted. The final version may differ from this version.

glucuronide conjugate metabolites present in plasma and urine. Again, previous pharmacokinetic studies of orally administered DIM in rodent models and human trials reported all DIM to be present as parent compound with no metabolites reported. Given that the [$^{14}$C]-BaP was a micro-dose (50 ng at T: 0), an impact on DIM metabolism or pharmacokinetics is extremely unlikely.

The DIM metabolites in plasma were sulfate and glucuronide conjugates of 3-methylenehydroxy-DIM, 2-ox-DIM, and 3-methylenehydroxy-2-ox-DIM. Lacking standards for conjugates, 3-methylenehydroxy-DIM (pyrano-DIM) or the di-hydroxylated metabolite, 3-methylenehydroxy-(pyrano)-2-ox-DIM, we are not reporting quantities but can report amounts of 2-ox-DIM and estimate pyrano-DIM (assuming the latter mono-hydroxylated metabolites elicits a similar ionization response from the mass spectrometer) in samples treated with β-glucuronidase/sulfatase. Pyrano-DIM is present at much higher levels than 2-ox-DIM. Appreciable amounts of the conjugated (and small amounts of the free) 3-methylenehydroxy-(pyrano)-2-ox-DIM, are also present in plasma.

In urine, not treated with deconjugation enzymes, there were significant amounts of the same sulfate and glucuronides observed in plasma with sulfate conjugates appearing to be dominant. As with resveratrol, the difference observed between sulfate and glucuronide conjugates may be partly due to a greater instrument response (area X/IS) to the sulfate (Muzzio et al., 2012). The ratio of sulfate/glucuronide may also be lower than predicted by instrument response, as assessed by the yield of 2-ox-DIM and 3-methylenehydroxy-2-ox-DIM, following incubation of urine samples with pure sulfatase or β-glucuronidase as well as β-glucuronidase containing sulfatase (Supplemental

DMD Fast Forward. Published on May 25, 2021 as DOI: 10.1124/dmd.120.000346
This article has not been copyedited and formatted. The final version may differ from this version.

Figure 2). As pyrano-DIM would be blocked from further oxygenation at the 2-position, and also could not be conjugated, the 3-methylenehydroxy-DIM must be stable long enough for the second oxygenation or conjugations by UGT and SULT to occur. We did not find any di-sulfate (exact mass 437.0119), di-glucuronide (exact mass 628.1551) or mixed sulfate and glucuronide metabolites in plasma or urine.

Our results strongly suggest robust metabolism of DIM in these subjects following oral administration (Figure 9), again, conflicting with previous studies in the literature. In an *in vitro* study with human MCF-7 breast cancer cells (Staub et al., 2006), incubation with DIM resulted in a metabolite pattern very similar to our present *in vivo* study although the hydroxylation and sulfation of DIM was not as robust. It took 48 hours of incubation with 1 μM [$^3$H]-DIM for levels of metabolites in media to exceed parent DIM. After 72 hours, in media 35% was present as DIM with the remainder sulfate conjugates whereas in the cell 81-93% of [$^3$H] was parent DIM perhaps indicating active transport of sulfate conjugates from MCF-7 cells. Staub et al. (2006) demonstrated, via the use of specific CYP1A2 inducers and inhibitors, that CYP1A2 was primarily responsible for initial hydroxylation. CYP1A2, unlike CYP1A1 and CYP1B1, is constitutively expressed at significant levels in liver as are numerous sulfotransferases and β-glucuronidases which may explain the robust first-pass metabolism (intestine may also play a role). I3C/DIM is known to induce hepatic CYP1A2 in rodents (Katchamart et al., 2000; Manson et al., 1997) and I3C supplementation (400-800 mg daily for 8 weeks) in women (measured as DIM *in vivo*), was effective in induction (4-fold) of CYP1A2 as determined by caffeine metabolism (Reed et al., 2005). Similarly, administration of resveratrol to humans at 1000 mg daily for 4 weeks resulted in induction of CYP1A2

DMD Fast Forward. Published on May 25, 2021 as DOI: 10.1124/dmd.120.000346
This article has not been copyedited and formatted. The final version may differ from this version.

activity (Chow et al., 2010). During human supplementation with DIM co-administration of inhibitors or inducers of CYP1A2 such as quercetin, resveratrol or caffeine could inhibit first-pass metabolism with possible resultant increased levels of parent DIM in plasma.

Given the robust metabolism, PBPK models developed in rodents (Anderton et al., 2004) may have to be modified for humans and further work on potential pharmacological properties of metabolites deserve attention. Staub et al., (2006) tested 2-ox-DIM as a potential ER ligand and found no activity. In this study 2-ox-DIM was effective in activating mouse AHR in a Hepa1 hepatoma cell line to a degree significantly greater than DIM and was comparable to the well-known tryptophan metabolites kynurenine, indole-3-aldehyde and indole-3-acetate (data not shown).

As the pharmacological activity of DIM metabolites has not previously been reported, a comparison to indole and 3-methylindole is useful. Indole (IND) and 2-ox-indole (2-ox-IND) are the major indoles found in both mouse and human feces and production in mice is entirely microbial (Dong et al., 2020). IND and 2-ox-IND are human selective AHR agonists but somewhat active in a Hepa1 reporter system (Dong et al., 2020). If 2-ox-DIM is also human AHR-selective the fact that we see significant AHR agonist activity with mouse AHR in Hepa1 cells suggest 2-ox-DIM would be even more active with human AHR. The potent mutagen and pulmonary toxicant, 3-methylindole (mIND), also produces 2-ox-mIND through CYP oxygenation, as well as hydroxylation at the 3-methyl position to generate I3C. 2-Ox-mIND formation is efficiently catalyzed by the CYP2A family (D'Agostino et al., 2009; Hartog et al., 2019) whereas CYP1A1, 1A2 and 1B1 are active in 3-methyl hydroxylation (Lanza and Yost, 2001).

DMD Fast Forward. Published on May 25, 2021 as DOI: 10.1124/dmd.120.000346
This article has not been copyedited and formatted. The final version may differ from this version.

*In vitro* studies with trout liver slices demonstrated that the relatively potent ($K_d$, low µM) estrogenic activity of DIM could be significantly blocked by the CYP inhibitor, SKF-525A (Shilling et al., 2001). This observation, along with those by our laboratory and others, demonstrating DIM is an inhibitor of multiple rat and humans CYPs (Parkin et al., 2008; Stresser et al., 1995a), raises the possibility that DIM metabolites, in addition to activating AHR, may exhibit significant drug (phytochemical)-drug interactions as seen with reduced tamoxifen metabolites in serum of women taking DIM long-term (Thomson et al., 2017). With respect to conjugates, SULT conjugation of 3-hydroxyindole produces the potent uremic toxicant indoxyl sulfate (Banoglu and King, 2002). The potential for sulfate or glucuronide metabolites of DIM to exhibit any pharmacological activity is not known.

A recently completed unpublished study (Dr. Emily Ho, Oregon State University and Drs. Cynthia A. Thomson and H.H. Sherry Chow, University of Arizona, personal communication) saw results (urine only) similar to the present study. Following 6 months of BR-DIM® 150 (twice daily to women) an untargeted metabolomics study demonstrated urine contained substantial amounts of glucuronide and sulfate conjugates of hydroxylated DIM.

In the present study we employed the commercially available BioResponse® 150 DIM supplement as it has been shown in clinical trials to have enhanced oral bioavailability in mice (Anderton et al., 2004). There is no rationale to expect that the BioResponse-DIM® 150 formulation (30% DIM in micro-encapsulation containing phosphatidylcholine and polyethylene glycol carriers to stimulate absorption) would be metabolized differently than pure DIM.

DMD Fast Forward. Published on May 25, 2021 as DOI: 10.1124/dmd.120.000346
This article has not been copyedited and formatted. The final version may differ from this version.

In addition to examination of a broader range of individuals *in vivo*, we plan to conduct *in vitro* studies with human intestinal and hepatic S9, as well as individually expressed CYPs, SULTs and UGTs followed by testing of metabolites for pharmacological activity to better understand the mechanism(s) of chemoprevention by DIM supplementation.

## Acknowledgments

The authors would like to thank Dr. Michael Zeligs of BioResponse L.L.C. for providing the BioResponse-DIM® 150 capsules used in this study. Dr. Stephen S. Hecht, University of Minnesota kindly provided us with [$^2H_2$]-DIM. Drs. Cynthia Thomson and H.H. Sherry Chow, University of Arizona, provided us with data on DIM metabolites in urine. Dr. Paul R. Blakemore, Department of Chemistry at Oregon State University provided the hypothesized pathway for formation of pyrano-DIM from 3-methylenehydroxy-DIM.

## Authorship Contributions

*Participated in research design:* Maier, Siddens, Uesugi, Tilton, Ho, Williams
*Conducted experiments:* Maier, Siddens, Uesugi, Choi, Leonard, Thomson, Pennington, Nguyen, Kolluri
*Performed data analysis:* Maier, Siddens, Choi, Leonard, Tilton, Smith, Williams, Nguyen, Kolluri
*Wrote or contributed to the writing of the manuscript:* Maier, Williams

## References

Aggarwal BB and Ichikawa H (2005) Molecular targets and anticancer potential of indole-3-carbinol and its derivatives. Cell Cycle 4: 1201-1215.

Ambrosone CB and Tang L (2009) Cruciferous vegetable intake and cancer prevention: role of nutrigenetics. Cancer Prev Res 2: 298-300.

Anderton MJ, Manson MM, Verschoyle R, Gescher A, Steward WP, Williams ML, and Mager DE (2004) Physiological modeling of formulated and crystalline 3,3'-diindolylmethane pharmacokinetics following oral administration in mice. Drug Metabol Disp 32: 632-638.

Ashrafian L, Sukhikh G, Kiselev V, Paltsev M, Drukh V, Kuznetsov I, Muyzhnek E, Apolikhina I, and Andrianova E (2015) Double-blind randomized placebo-controlled multicenter clinical trial (phase IIa) on diindolylmethane's efficacy and safety in the treatment of CIN: Implications for cervical cancer prevention. EPMA J 6:25.

Auborn KJ, Fan S, Rosen EM, Goodwin L, Chandreskaren A, Williams DE, Chen D, and Carter TH (2003) Indole-3-carbinol is a negative regulator of estrogen. Nutritional genomics and proteomics in cancer prevention. J Nutr (Suppl). 133S: 1S-6S.

Baenas N, Suárez-Martínez C, García-Viguera C, and Moreno DA (2017) Bioavailability and new biomarkers of cruciferous sprouts consumption. Fd Res Intl 100: 497-503.

Banoglu B and King RS (2002) Sulfation of indoxyl by human and rat aryl (phenol) sulfotransferases to form indoxyl sulfate. Eur J Drug Metabol Pharmacokinet 27: 135-140.

Bjeldanes LF, Kim J-Y, Grose KR, Bartholomew JC, and Bradfield CA (1991) Aromatic hydrocarbon responsiveness-receptor agonists generated from indole-3-carbinol *in vitro* and *in vivo*: Comparisons with 2,3,7,8-tetrachlorodibenzo-*p*-dioxin. Proc Natl Acad Sci (USA) 88: 9543-9547.

Bonnesen C, Eggleston IM, and Hayes JD (2001) Dietary indoles and isothiocyanates that are generated from cruciferous vegetables can both stimulate apoptosis and confer protection against DNA damage in human colon cell lines. Cancer Res 61: 6120-6130.

Bradfield CA, and Bjeldanes LF (1987a) High-performance liquid chromatographic analysis of anticarcinogenic indoles in Brassica oleracea. J Ag Fd Chem 35: 46-49.

Bradfield CA, and Bjeldanes LF (1987b) Structure-activity relationships of dietary indoles: A proposed mechanism of action as modifiers of xenobiotic metabolism. J Toxicol Environ Hlth 21: 311-323.

Bradlow HL (2008) Indole-3-carbinol as a chemoprotective agent in breast and prostate cancer. In Vivo 22: 441-446.

Chow H-H, Garland LL, Hsu C-H, Vining DR, Chew WM, Miller JA, Perloff M, Crowell JA, and Alberts DS (2010) Resveratrol modulates drug- and carcinogen-metabolizing enzymes in a healthy volunteer study. Cancer Prev Res 3: 1169-1175.

D'Agostino J, Zhuo X, Shadid M, Morgan DG, Zhang X, Humphreys WG, Shu Y-Z, Yost GS and Ding X (2009) The pneumotoxin 3-methylindole is a substrate and a mechanism-based inactivator of CYP2A13, a human cytochrome P450 enzyme preferentially expressed in the respiratory tract. Drug Metabol Disp 37: 2018-2027.

Dalessandri KM, Firestone GL, Fitch MD, Bradlow HL, and Bjeldanes LF (2004) Pilot study: Effect of 3,3'-diindolylmethane supplements on urinary hormone metabolites in postmenopausal women with a history of early-stage breast cancer. Nutr Cancer 50: 161-167.

Dong F, Hao F, Murray IA, Smith PB, Koo I, Tindall AM, Kris-Etherton PM, Gowda K, Amin SG, Patterson AD and Perdew GH (2020) Intestinal microbiota-derived tryptophan metabolites are predictive of Ah receptor activity. Gut Microbes 12 :1, 1788899.

Donovan MG, Selmin OI, and Romagnolo DF (2018) Aryl hydrocarbon receptor diet and breast cancer risk. Yale J Biol Med 91: 105-127.

Faust D, Nikolova T, Wätjen W, Kaina B. and Dietrich C (2017) The Brassica-derived phytochemical indolo[3,2-b]carbazole protects against oxidative DNA damage by aryl hydrocarbon receptor activation. Arch Toxicol 91: 967-982.

Firestone GL and Bjeldanes LF (2003) Indole-3-carbinol and 3-3'-diindolylmethane antiproliferative signaling pathways control cell-cycle gene transcription in human breast cancer cells by regulating promoter-Sp1 transcription faction interactions. J Nutr 133: 2448S-2455S.

Fujioka N, Ainslie-Waldman CE, Upadhyaya P, Carmella SG, Fritz VA, Rohwer C, Fan Y, Rauch D, Le C, Hatsukami DK, and Hecht SS (2014) Urinary 3,3'-diindolylmethane: A biomarker of glucobrassicin exposure and indole-3-carbinol uptake in humans. Cancer Epidemiol Biomarkers Prev 23: 282-287.

DMD Fast Forward. Published on May 25, 2021 as DOI: 10.1124/dmd.120.000346
This article has not been copyedited and formatted. The final version may differ from this version.

Fujioka N, Fritz V, Upadhyaya P, Kassie F, and Hecht SS (2016) Research on cruciferous vegetables, indole-3-carbinol and cancer prevention. A tribute to Lee W. Wattenberg. Molec Nutr Fd Res 60: 1228-1238.

Gibaldi M, and Perrier D (1982) Pharmacokinetics, M. Dekker, New York.

Hartog M, Zhang Q-Y and Ding X (2019) Role of mouse cytochrome P450 enzymes of the *Cyp2abfgs* subfamilies in the induction of lung inflammation by cigarette smoke exposure. Toxicol Sci 172 :123-131.

Hayes JD, Kelleher MO, and Eggleston IM (2008) The cancer chemopreventive actions of phytochemicals derived from glucosinolates. Eur J Nutr 47: 73-88.

Heath EI, Heilbrun LK, Li J, Vaishampayan U, Harper F, Pemberton P, and Sarkar FH (2010) A phase 1 dose-escalation study of oral BR-DIM (BioResponse 3,3'-diindolylmethane) in castrate-resistant, non-metastatic prostate cancer. Am J Transl Res 2: 402-411.

Higdon JV, Delage B, Williams DE, and Dashwood RH (2007) Cruciferous vegetables and human cancer risk: Epidemiologic evidence and mechanistic basis. Pharmacol Res 55: 224-236.

Hsu EL, Chen N, Westbrook A, Wang F, Zhang R, Taylor RT, and Hankinson O (2008) CXCR4 and CXCL12 down-regulation: A novel mechanism for the chemoprotection of 3,3'-diindolylmethane for breast and ovarian cancers. Cancer Lett 265: 113-123.

Hwang C, Sethi S, Heibrun LK, Gupta NS, Chitale DA, Sakr WA, Menon M, Peabody JO, Smith DW, Sarkar FH, and Heath EI (2016) Anti-androgenic activity of absorption-enhanced 3,3'-diindolylmethane in prostatectomy patients. Am J Transl Res 8: 166-176.

Jellinck PH, Forkert PG, Riddick DS, Okey AB, Michnovicz JJ, and Bradlow HL (1993) Ah receptor binding properties of indole carbinols and induction of hepatic estradiol hydroxylation. Biochem Pharmacol 45: 1129-1136.

Katchamart S, Stresser DS, Dehal SS, Kupfer D, and Williams DE (2000) Concurrent flavin-containing monooxygenase down regulation and cytochrome P-450 induction by dietary indoles in the rat: Implications for drug-drug Interactions. Drug Metabol Dispos 28: 930-936.

Kim YS and Milner JA (2005) Targets for indole-3-carbinol in cancer chemoprevention. J Nutr Biochem 16: 65-73.

Kim MK and Park JHY (2009) Cruciferous vegetable intake and the risk of human cancer: Epidemiology evidence. Proc Nutr Soc 68: 103-110.

Lampe JW, Chen C, Li S, Prunty J, Grate MT, Meehan DF, Barale KV, Dightman DA, Feng Z, and Potter JD (2000) Modulation of human glutathione S-transferases by botanically defined vegetable diets. Cancer Epid Biomarkers Prev 9: 787-793.

Lanza DL and Yost GS (2001) Selective dehydrogenation/oxygenation of 3-methylindole by cytochrome P450 enzymes. Drug Metabol Dispos 29: 950-953.

Li Y, and Sarkar FH (2015) Role of BioResponse 3,3'-diindolylmethane in the treatment of human prostate cancer: Clinical experience. Med Princ Pract 25(Suppl 2): 11S-117S.

Lord RS, Bongiovanni B, and Bralley JA (2002) Estrogen metabolism and the diet-cancer connection: Rationale for assessing the ratio of urinary hydroxylated estrogen metabolites. Altern Med Rev 7: 112-129.

Madeen E, Siddens LK, Uesugi S, McQuistan T, Corley RC, Smith J, Waters KM, Tilton SC, Anderson KA, Ognibene T, Turteltaub K, and Williams DE (2019) Toxicokinetics of benzo[*a*]pyrene in humans: extensive metabolism as determined by UPLC-accelerator mass spectrometry following oral micro-dosing. Toxicol Appl Pharmacol 364: 97-105.

Manson MM, Ball HWL, Barrett MC, Clark HL, Judah DJ, Williamson G, and Neal GE (1997) Mechanism of action of dietary chemoprotective agents in rat liver: Induction of phase I and II drug metabolizing enzymes and aflatoxin $B_1$ metabolism. Carcinogenesis 18: 1729-1738.

Marconett CN, Sundar SN, Poindexter KM, Stueve TR, Bjeldanes LF, and Firestone GL (2010) Indole-3-carbinol triggers aryl hydrocarbon receptor-dependent estrogen receptor (ER)alpha protein degradation in breast cancer cells disrupting an ERalpha-GATA3 transcriptional cross-regulatory loop. Mol Biol Cell 21: 1166-1177.

Maruthanila VL, Poornima J, and Mirunalini S (2014) Attenuation of carcinogenesis and the mechanism underlying by the influence of indole-3-carbinol and its metabolite 3,3'-diindolylmethane: A therapeutic marvel. Adv Pharmacol Sci 2014: 832161.

Minich DM, and Bland JS (2007) A review of the clinical efficacy and safety of cruciferous vegetable phytochemicals. Nutr Rev 65: 259-267.

Muzzio M, Huang Z, Hu S-C, Johnson WD, McCormick DL, and Kapetanovic IM (2012) Determination of resveratrol and its sulfate and glucuronide metabolites in plasma by LC-MS/MS and their pharmacokinetics in dogs. J Pharm Biomed Anal 59: 201-208.

Navarro SL, Peterson S, Chen C, Makar KW, Schwarz Y, King IB, Li SS, Kestin M, and Lampe JW (2009) Cruciferous vegetable feeding alters UGT1A1 activity: Diet- and genotype-dependent changes in serum bilirubin in a controlled feeding trial. Cancer Prev Res 2: 345-352.

Paltsev M, Kiselev V, Muyzhnek E, Drukh V, Kuznetsov I, and Pchelintseva O (2013) Comparative preclinical pharmacokinetics study of 3,3'-diindolylmethane formulations: Is personalized treatment and targeted chemoprevention in the horizon? EPMA J 4:25.

Paltsev M, Kiselev V, Drukh V, Muyzhnek E, Kuznetsov I, Andrianova E, and Pchelintseva O (2016) First results of the double-blind randomized placebo-controlled multicenter clinical trial of DIM-based therapy designed as a personalized approach to reverse prostatic intraepithelial neoplasia. EPMA J 7:5.

Parkin DR, Lu Y, Bliss RL, and Malejka-Giganti D (2008) Inhibitory effects of a dietary phytochemical 3,3'-diindolylmethane on the phenobarbital-induced hepatic CYP mRNA expression and CYP-catalyzed reactions in female rats. Fd Chem Toxicol 46: 2451-2458.

Peterson S, Schwarz Y, Li SS, Li L, King IB, Chen C, Eaton DL, Potter JD, and Lampe JW (2009) CYP1A2, GSTM1, and GSTT1 polymorphisms and diet effects on CYP1A2 activity in a crossover feeding trial. Cancer Epidem Biomarkers Prev 18: 3118-3125.

Pillaiyar T, Köse M, Sylvester K, Weighardt H, Thimm D, Borges G, Förster I, von Kügelgen I, and Müller CE (2017) Diindolylmethane derivatives: Potent agonists of the immunostimulatory orphan G Protein-Coupled Receptor GPR84. J Med Chem 60: 3636-3655.

Rajoria S, Suriano R, Wilson YL, Schantz SP, Moscatello A, Geliebter J, and Tiwari RK (2011) 3,3'-Diindolylmethane inhibits migration and invasion of human cancer cells through combined suppression of ERK and AKT pathways. Oncol Rep 25: 491-497.

Rannug A, Rannug U, Rosenkranz HS, Winqvist L, Westerhom R, Agurell E, and Grafstrom AK (1987) Certain photo-oxidized derivatives of tryptophan bind with very high affinity to the Ah receptor and are likely to be endogenous signal substances. J Biol Chem 262: 15422-15427.

Reed GA, Arneson DW, Putnam WC, Smith HJ, Gray JC, Sullivan DK, Mayo MS, Crowell JA, and Hurwitz A (2006) Single-dose and multiple-dose administration of indole-3-carbinol to women: Pharmacokinetics based on 3,3'-diindolylmethane. Cancer Epidemiol Biomarkers Prev 15: 2477-2481.

Reed GA, Peterson KS, Smith HJ, Gray JC, Sullivan DK, Mayo MS, Crowell JA, and Hurwitz A (2005) A phase 1 study of indole-3-carbinol in women: Tolerability and effects. Cancer Epidemiol Biomarkers Prev 14: 1953-1960.

Reed GA, Sunega JM, Sullivan DK, Gray JC, Mayo MS, Crowell JA, and Hurwitz A (2008) Single-dose pharmacokinetics and tolerability of absorption-enhanced 3,3'-diindolylmethane in healthy subjects. Cancer Epidem Biomarkers Prev 17: 2619-2624.

Sepkovic DW, Bradlow HL, and Bell M (2001) Quantitative determination of 3,3'-diindolylmethane in urine of individuals receiving indole-3-carbinol. Nutr Cancer 41: 57-63.

Shilling AD, Carlson DB, Katchamart S, and Williams DE (2001) 3,3'-Diindolylmethane, a major condensation product of indole-3-carbinol, is a potent estrogen in the rainbow trout. Toxicol Appl Pharmacol 170: 191-200.

Shorey LE, Madeen EP, Atwell LL, Ho E, Löhr CV, Pereira CB, Dashwood RH, and Williams DE (2013) Differential modulation of dibenzo[*def,p*]chrysene transplacental carcinogenesis: Maternal diets rich in indole-3-carbinol versus sulforaphane. Toxicol Appl Pharmacol 270: 60-69.

Staub RE, Onisko B, and Bjeldanes LF (2006) Fate of 3,3'-diindolylmethane in cultured MCF-7 human breast cancer cells. Chem Res Toxicol 19: 436-442.

Stresser DM, Bailey GS, and Williams DE (1994a) Indole-3-carbinol and β-naphthoflavone induction of cytochromes P450 associated with bioactivation and detoxication of aflatoxin $B_1$ in the rat. Drug Metabol Dispos 22: 383-391.

Stresser DM, Bjeldanes LF, Bailey GS, and Williams DE (1995a) The anticarcinogen 3,3'-diindolylmethane is an inhibitor of cytochrome P-450. J Biochem Toxicol 10: 191-201.

Stresser DM, Williams DE, McLellan LI, Harris TM, and Bailey GS (1994b) Indole-3-carbinol induces a rat liver glutathione transferase subunit (Yc2) with high activity towards aflatoxin $B_1$ *exo*-epoxide: Association with reduced levels of hepatic $AFB_1$-DNA adducts *in vivo*. Drug Metabol Dispos 22: 392-399.

Stresser DM, Williams DE, Griffin DA, and Bailey GS (1995b) Mechanisms of tumor modulation by indole-3-carbinol. Disposition and excretion of [$^3$H]-indole-3-carbinol in male Fischer 344 rats. Drug Metabol Dispos 23: 965-975.

Takahashi N, Stresser DM, Williams DE, and Bailey GS (1995) Induction of hepatic CYP1A by indole-3-carbinol in protection against aflatoxin $B_1$ hepatocarcinogenesis in rainbow trout. Fd Chem Toxicol 33: 841-850.

Thomson CA, Chow HHS, Wertheim BC, Roe DJ, Stopeck A, Maskarinec G, Altbach M, Chalasani P, Huang C, Strom MB, Galons J-P, and Thompson PA (2017) A randomized, placebo-controlled trial of diindolylmethane for breast cancer biomarker modulation in patients taking tamoxifen. Breast Cancer Res Treat 165: 97-107.

Thomson CA, Ho E, and Strom MB (2016) Chemopreventive properties of 3,3'-diindolylmethane in breast cancer: evidence from experimental and human studies. Nutr Rev 74: 432-443.

van Poppel G, Verhoeven DT, Verhagen H, and Goldbohm RA (1999) Brassica vegetables and cancer prevention. Epidemiology and mechanisms. Adv Exp Med Biol 472: 159-168.

Walters DG, Young PJ, Agus C, Knize MG, Boobis AR, Gooderham NJ, and Lake BG (2004) Cruciferous vegetable consumption alters the metabolism of the dietary carcinogen 2-amino-1-methyl-6-phenylimidazo[4,5-*b*]pyridine (PhIP) in humans. Carcinogenesis 25: 1659-1669.

Wattenberg LW, and Loub WD (1978) Inhibition of polycyclic aromatic hydrocarbon-induced neoplasia by naturally occurring indoles. Cancer Res 38: 1410-1413.

Weng, J-R, Tsai C-H, Kulp SK, and Chen C-S (2008) Indole-3-carbinol as a chemopreventive and anti-cancer agent. Cancer Lett 262: 153-163.

DMD Fast Forward. Published on May 25, 2021 as DOI: 10.1124/dmd.120.000346
This article has not been copyedited and formatted. The final version may differ from this version.

**Footnotes:** This study was funded by Public Health Service NIH grants P42ES016465, R01ES028600, T32ES07060, P30ES030287, P30CA23074, and Multi-State NIFA projects W4002 and W4122 from the Oregon Agricultural Experiment Station. The authors have no conflict of interest to declare.

DMD Fast Forward. Published on May 25, 2021 as DOI: 10.1124/dmd.120.000346
This article has not been copyedited and formatted. The final version may differ from this version.

## Figure Legends

**Figure 1. Quantitation of DIM and Hydroxylated Metabolites in Plasma by UPLC-MS/MS Following Deconjugation.** Top Panels: DIM and 2-ox-DIM standards; DIM (m/z 246.95>130.15), 0.25 pmol with instrument response with standards on right; 2-ox-DIM (m/z 263.12→130.15), 0.5 pmol with instrument response with standards on right; Bottom Panel, UPLC of plasma extract from a single individual at T= 0 hour. One mL of plasma was adjusted to pH 5.0 and treated with β-glucuronidase and sulfatase. Following an overnight incubation the extract was analyzed by UPLC-MS/MS as described in Materials and Methods.

**Figure 2. MS/MS spectrum of mono-oxygenated DIM at m/z 263.1179.** The fragmentation pattern for the oxygenated product of DIM was obtained from A. the 2-ox-DIM standard; B. the peak corresponding to the retention time of the 2-ox-DIM standard from an extract from urine; C. proposed oxygenated DIM distinct from 2-ox-DIM from urine (3-methylenehydroxy-DIM or pyrano-DIM) with specific fragment ion m/z 146.0596.

**Figure 3. Plasma Levels of DIM, 2-ox-DIM and Pyrano-DIM Over Time.** Blood was collected from each of the 7 individuals at time points indicated. Plasma was isolated, treated with sulfatase/β-glucuronidase, extracted and analyzed by UPLC-MS/MS as described in Material and Methods. DIM and 2-ox-DIM were quantified utilizing standard curves; pyrano-DIM was estimated based on instrument response with 2-ox-DIM.

**Figure 4. Plasma Levels of Sulfate and Glucuronide Conjugates of Mono- and Di-Hydroxylated DIM and Free Di-Hydroxylated-DIM**. Blood was collected from the 7 individuals at the time points indicated. Plasma was isolated, extracted and analyzed by UPLC-MS/MS as described in materials and methods. Bars indicate the mean (n=7) peak area of instrument response and the bars the S.D.

**Figure 5. Urine Levels of DIM, 2-ox-DIM and 3-Methylenehydroxy(Pyrano)-DIM Over Time.** All urine was collected over 48 hours post-dosing and pooled in fractions of 0-6, 6-12, 12-24 and 24-48 hours. Aliquots of 1 mL were treated with sulfatase/β-glucuronidase, extracted and analyzed by UPLC-MS/MS as described in Materials and Methods. No DIM or DIM metabolites were seen prior to initiation of 1 week of DIM supplementation (-7d). The 0 hour time point was urine collected just prior to the last dose (morning of day 8). Bars indicate the mean (n=7) in pmol/mg creatinine and the bars the S.D. DIM and 2-ox-DIM were quantified utilizing standard cures; pyrano-DIM (from 3-methylenehydroxy-DIM) was estimated based on instrument response with 2-ox-DIM standards.

**Figure 6. Sulfate Conjugates of Mono- and Di-Hydroxylated DIM Metabolites in Urine.** One 1 mL aliquots of urine collected from a single individual (BaP022), 6-12 hours post-dosing, was treated with sulfatase, extracted and analyzed by UPLC-MS/MS as described in Materials and Methods. The molecular ions exhibited m/z values of 343.0731 (peak eluting at 4.585 minutes) for the sulfate conjugate of mono-

DMD Fast Forward. Published on May 25, 2021 as DOI: 10.1124/dmd.120.000346
This article has not been copyedited and formatted. The final version may differ from this version.

hydroxylated DIM and 359.0686 for the sulfate conjugates of di-hydroxylated-DIM (peaks eluting at 3.550 and 3.867 minutes. The fragment ion at 146.0596 is diagnostic for pyrano(3-methylenehydroxy)-DIM and is not seen with 2-ox-DIM.

**Figure 7. Glucuronide Metabolites of Mono-Hydroxylated DIM**. One 1 mL aliquots of urine collected from a single individual (BaP022) 6-12 hours post-dosing was treated with β-glucuronidase, extracted and analyzed by UPLC-MS/MS as described in Materials and Methods. The peak eluting at 3.682 minutes exhibited an m/z value of 439.1743. The fragment ion at 146.0596 is diagnostic for pyrano(3-methylenehydroxy)-DIM and is not seen with 2-ox-DIM.

**Figure 8. AHR Activation in a Hepa1 Reporter System by DIM and 2-ox-DIM.** DIM and 2-ox-DIM were incubated with a mouse hepatoma cell line (Hepa1) with an XRE-containing luciferase reporter in a 96 well plate. FICZ was included as a positive control. Test compounds (in 0.1% DMSO) were added to 200 µL of media in wells and incubated for 18-24 hours prior to analyzing luciferase activity as reported in Materials and Methods. The bars are the mean of triplicates (± SD). Significant differences between identical concentrations of DIM and 2-ox-DIM were determined with a two-tail t test and are indicated by *($p<0.05$).

**Figure 9. Phase 1 (CYP) and Phase 2 (UGT and SULT) of DIM in Humans.** The pathway for formation of two mono-oxygenated metabolites and one di-oxygenated metabolite is shown with subsequent conjugation by UGT and SULT. The identity of the 2-ox-DIM is confirmed with a synthesized standard. The second hydroxylated metabolite is tentatively identified as 3-methylenehydroxy-DIM which spontaneously is converted to a pyrano product. The di-oxygenated product is tentatively identified as 3-methylenehydroxy-2-ox-DIM. Highlighted figure on right is the proposed pathway for spontaneous conversion of 3-methylenehydroxy-DIM to pyrano-DIM.

DMD Fast Forward. Published on May 25, 2021 as DOI: 10.1124/dmd.120.000346
This article has not been copyedited and formatted. The final version may differ from this version.

**Table 1. Volunteer Demographics**

| Volunteer | Age | Sex | BMI at screening visit | Race | Hispanic (Y/N) |
|---|---|---|---|---|---|
| BaP021 | 27 | M | 24.3 | White | N |
| BaP022 | 65 | M | 32.5 | White | N |
| BaP025 | 44 | M | 27.5 | White | N |
| BaP028 | 49 | M | 28.1 | White | N |
| BaP031 | 59 | F | 33.7 | White | N |
| BaP041 | 26 | M | 22.4 | Black/AA | N |
| BaP042 | 43 | M | 37.4 | White | N |

**Table 2A. Individual Pharmacokinetics of DIM, 2-Ox-DIM plus Pyrano-DIM (3-Methylenehydroxy-DIM): Non-Compartmental Model**

| Volunteer | $T_{max}$ (hr) DIM | $T_{max}$ (hr) OH-DIM[1] | $C_{max}$ (pmol/mL) DIM | $C_{max}$ (pmol/mL) OH-DIM[2] | $AUC_{0-48hr}$ (pmol x hr x $mL^{-1}$) DIM | $AUC_{0-48hr}$ (pmol x hr x $mL^{-1}$)[2] OH-DIM | $T_{1/2}$ (hr) DIM | $T_{1/2}$ (hr) OH-DIM[1,3] | Cl (L/hr) DIM[1] | $V_{dis}$ (L) DIM[1] |
|---|---|---|---|---|---|---|---|---|---|---|
| BaP021 | - | 0.25 | - | 4230 | - | 11,100 | - | 9.84 | - | - |
| BaP022 | 4.0 | 8 | 265 | 205 | 2890 | 2740 | 4.13 | 8.36 | 127 | 759 |
| BaP025 | 1.5 | 1.5 | 1770 | 8280 | 4190 | 16,600 | 3.87 | 5.12 | 87.7 | 490 |
| BaP028 | 3.0 | 3.0 | 362 | 290 | 2990 | 4510 | 3.76 | 14.1 | 123 | 669 |
| BaP031 | 3.0 | 3.0 | 380 | 184 | 5020 | 2910 | 8.85 | 11.9 | 73.3 | 937 |
| BaP041 | 1.5 | 2.0 | 68 | 125 | 72 | 1500 | 1.22 | 6.14 | - | - |
| BaP042 | 3.0 | 3.0 | 120 | 80 | 935 | 699 | 3.92 | 9.93 | 393 | 2220 |
| | 2.67 ± 0.98 | 2.96 ± 2.44 | 423 ± 610 | 1910 ± 3190 | 2300 ± 2000 | 5730 ± 5900 | 4.29 ± 2.48 | 9.34 ± 3.13 | 161 ± 132 | 1010 ± 693 |

[1]The reported $T_{max}$ is for pyrano-DIM

[2]The reported $C_{max}$ and $AUC_{0-48hr}$ are for the sum of 2-ox-DIM and pyrano-DIM

**Table 2B. Individual Pharmacokinetics of DIM: One-Compartmental Model**

| Volunteer | $K_a$ $hr^{-1}$ DIM | $K_{1e}$ $hr^{-1}$ DIM | $V_1$ (L) DIM | $T_{1/2}$ (hr) DIM |
|---|---|---|---|---|
| BaP021 | - | - | - | - |
| BaP022 | 0.28 | 0.28 | 513 | 2.45 |
| BaP025 | 0.70 | 0.70 | 222 | 0.99 |
| BaP028 | 0.18 | 0.84 | 166 | 0.82 |
| BaP031 | 0.08 | 1.16 | 72.1 | 0.60 |
| BaP041 | - | - | - | - |
| BaP042 | 0.29 | 0.29 | 1490 | 2.37 |
| | 0.30 ± 0.23 | 0.65 ± 0.37 | 492 ± 580 | 1.45 ± 0.89 |

[1]The reported $T_{max}$ is for pyrano-DIM

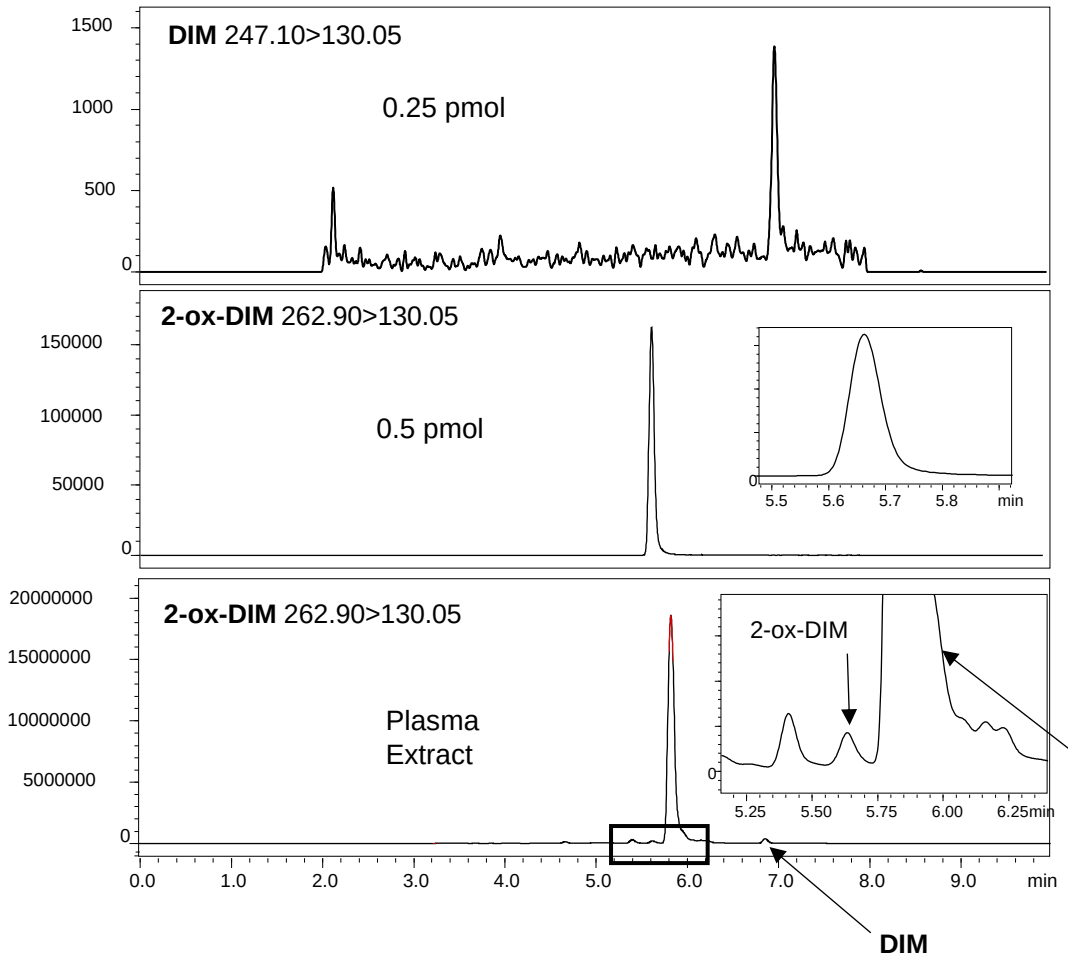


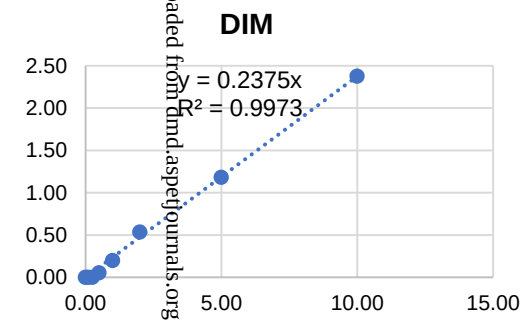


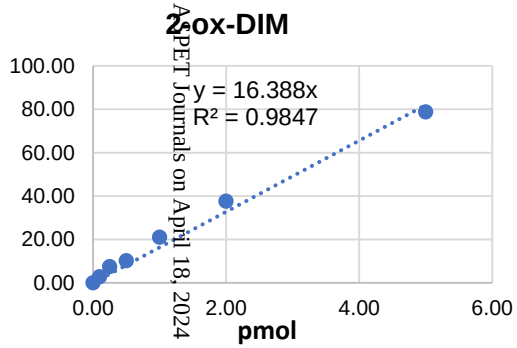


**3-methylenehydroxy-DIM or pyrano-DIM**

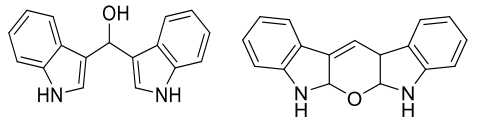




# Figure 1

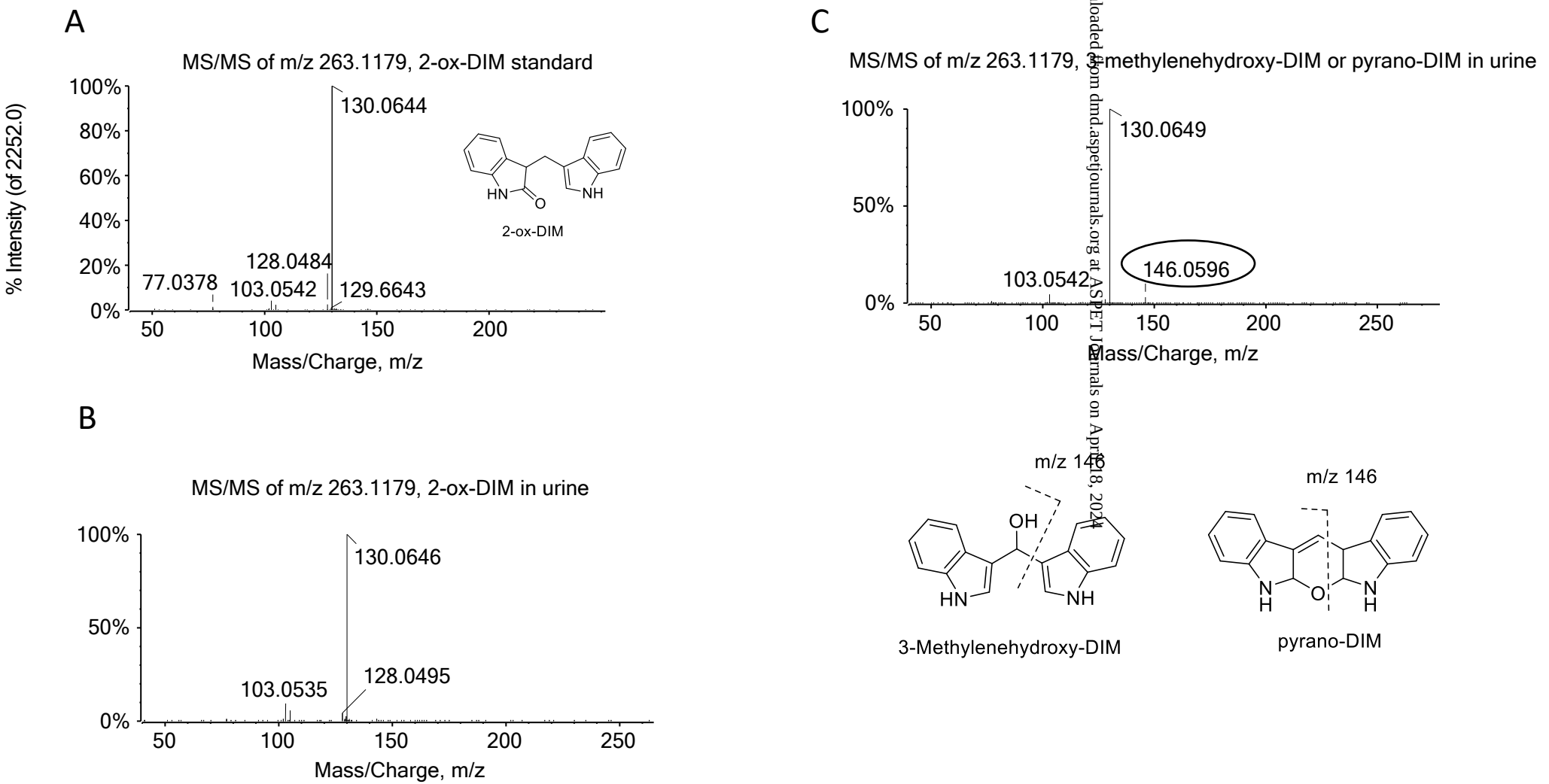




**Figure 2**

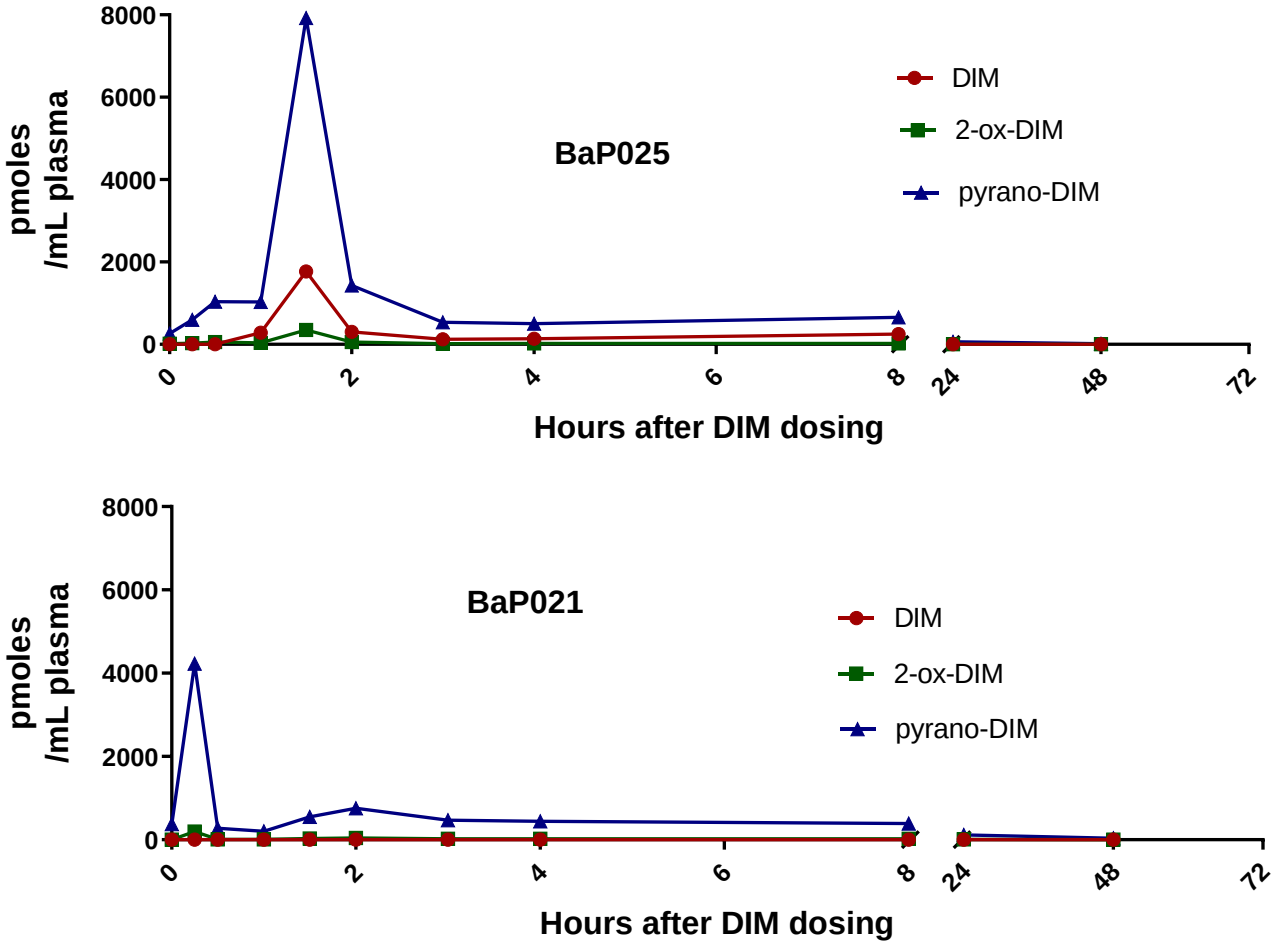


**Figure 3**

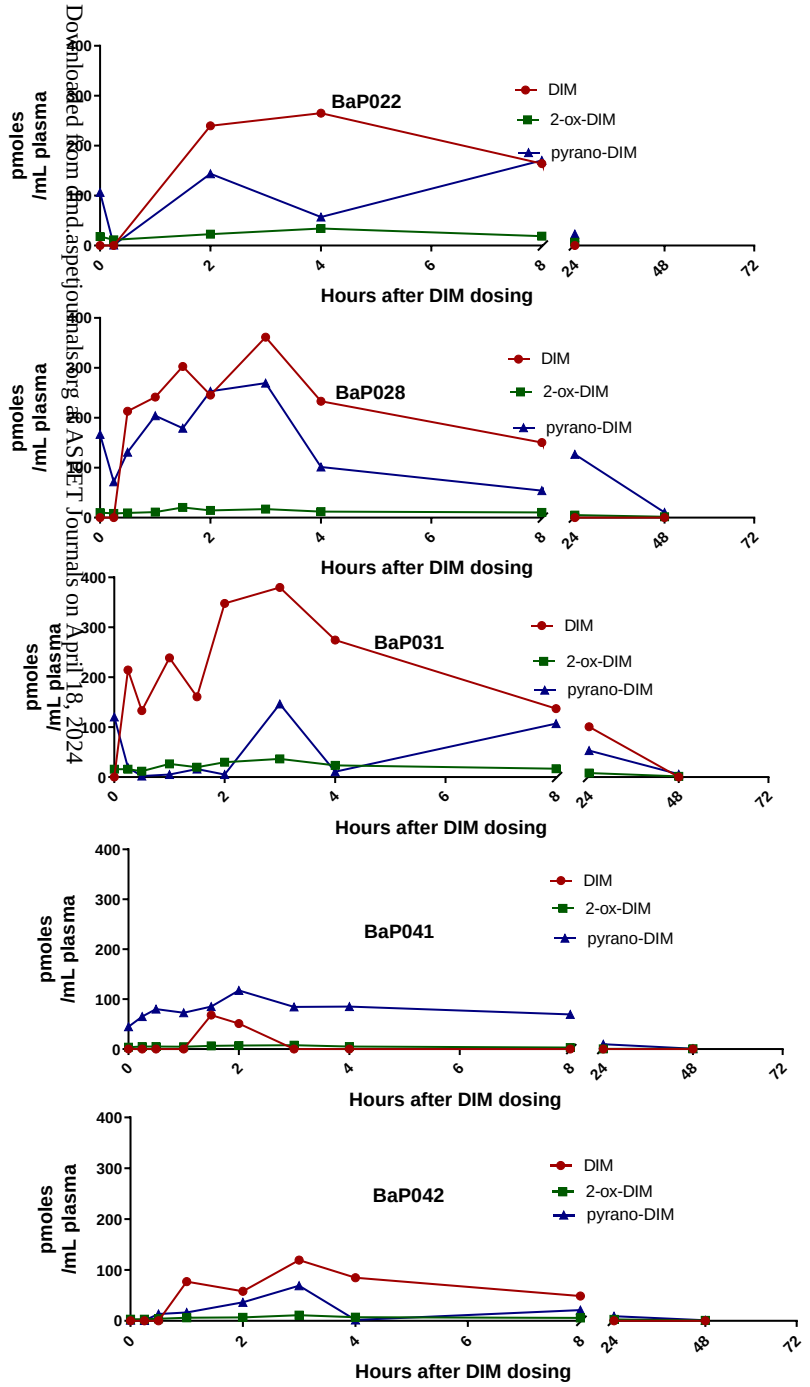

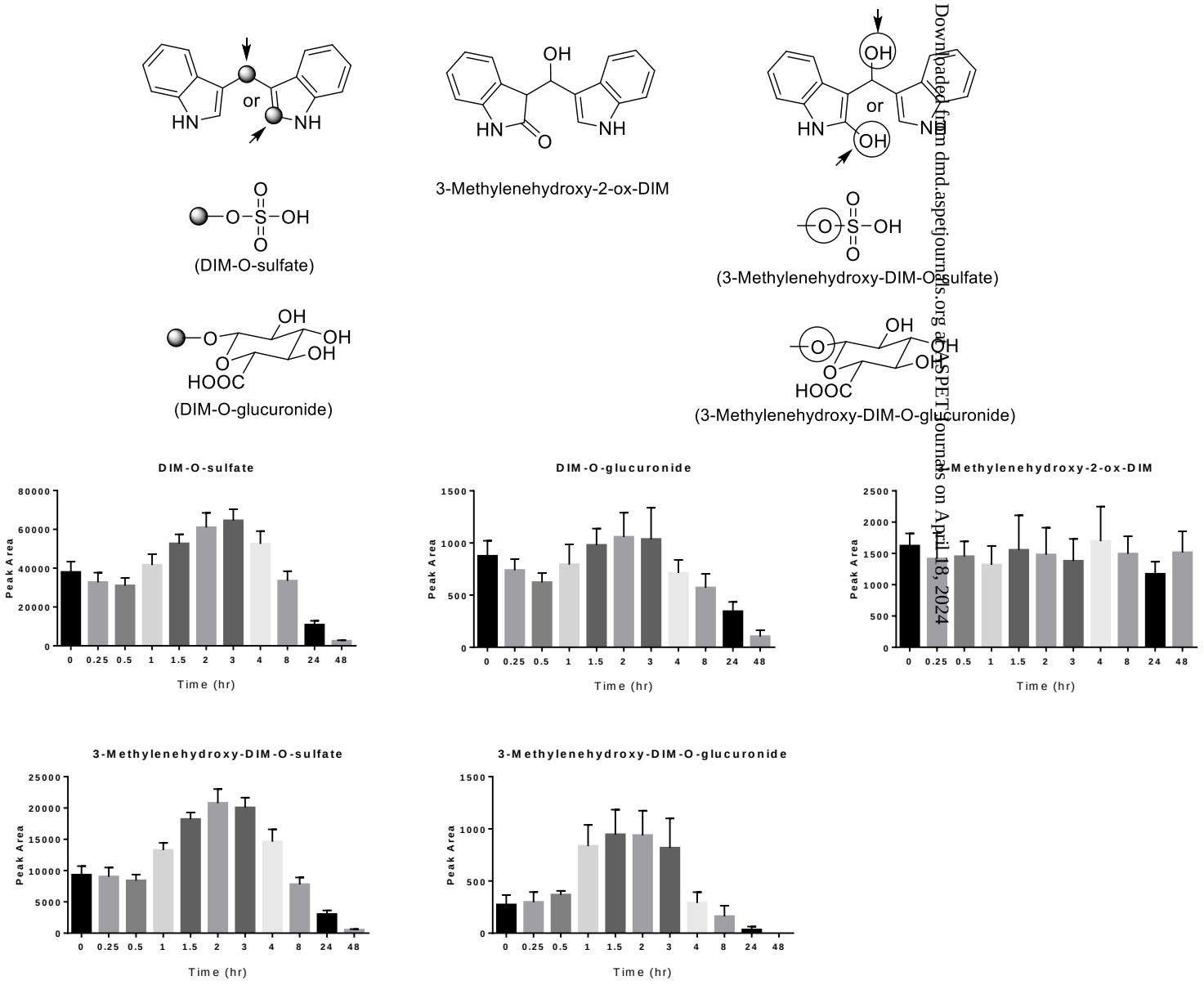


**Figure 4**

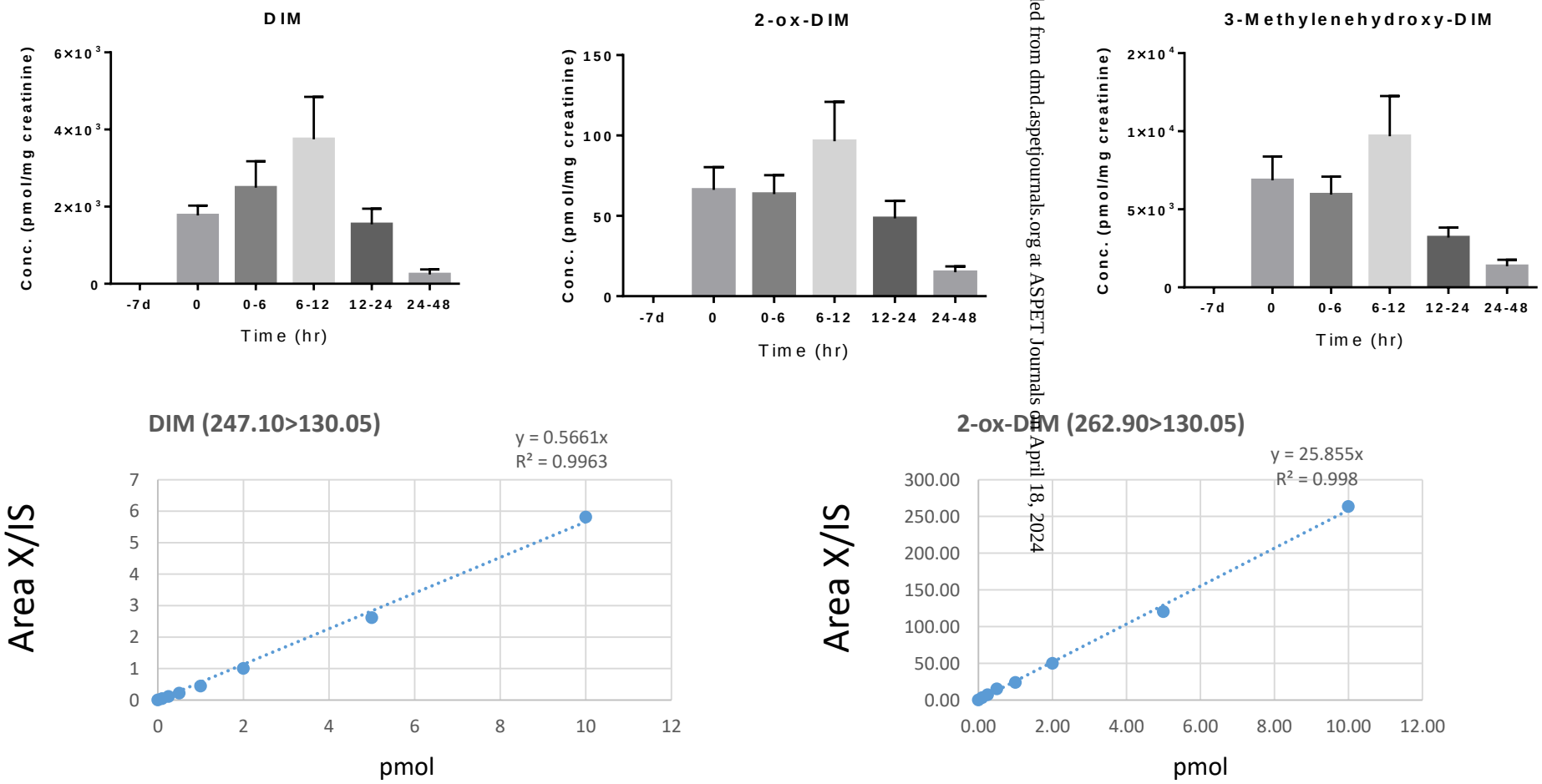


**Figure 5**

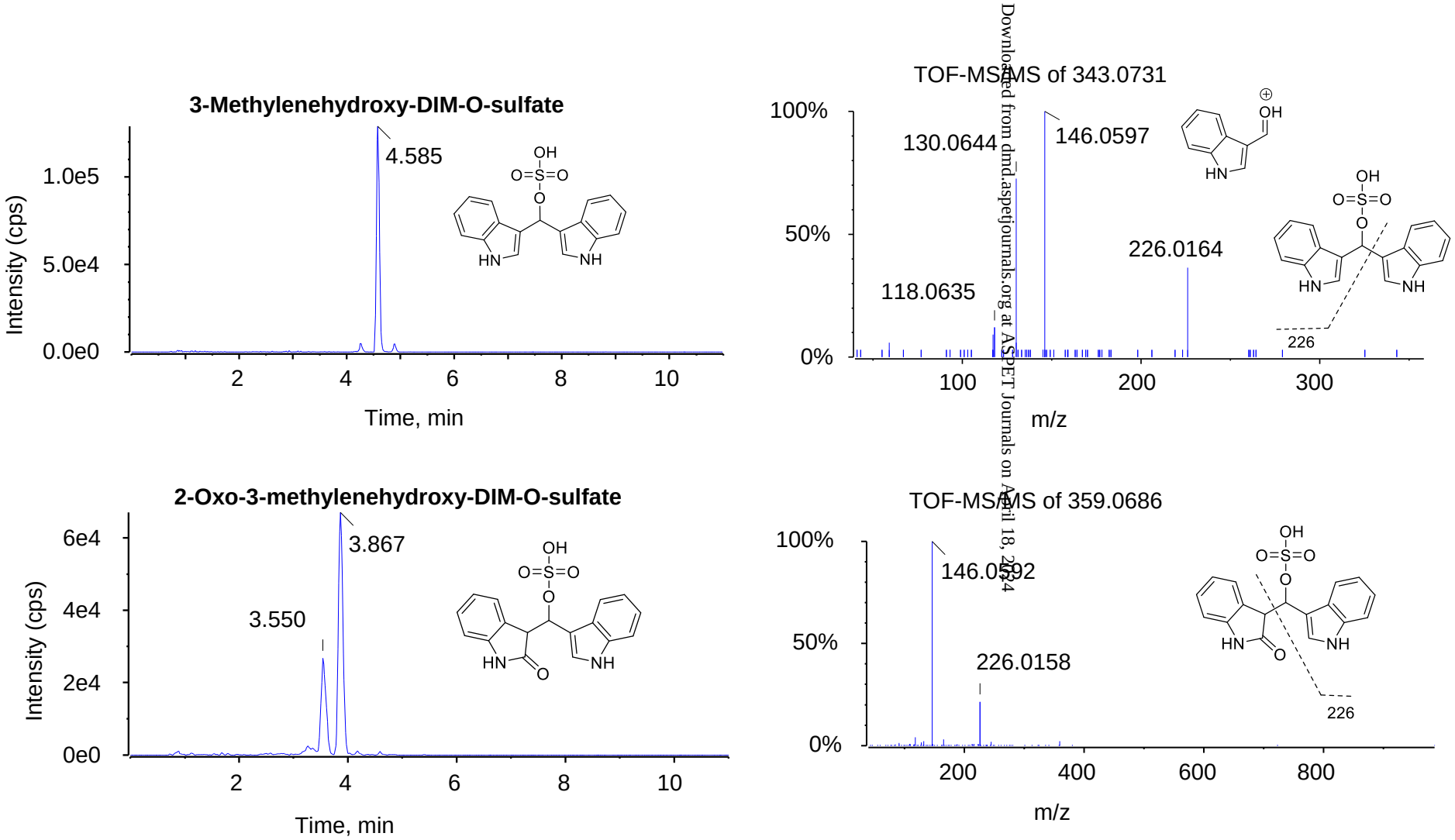




**Figure 6**

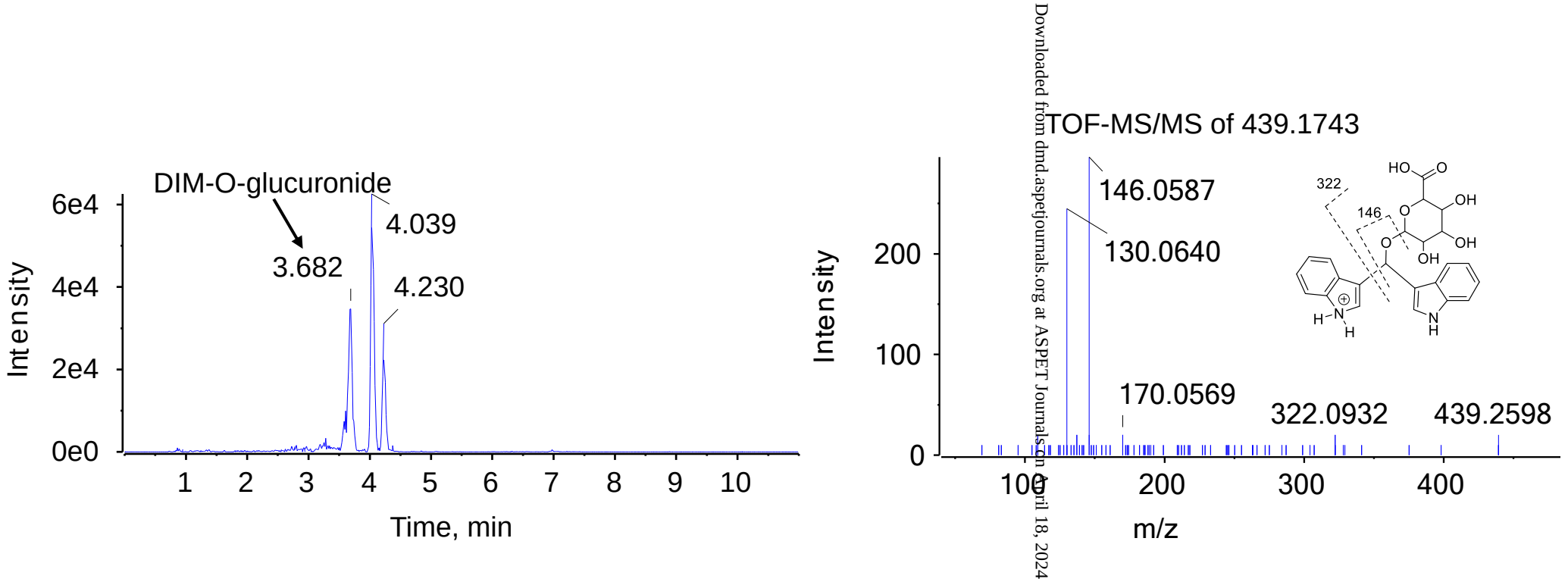




**Figure 7**

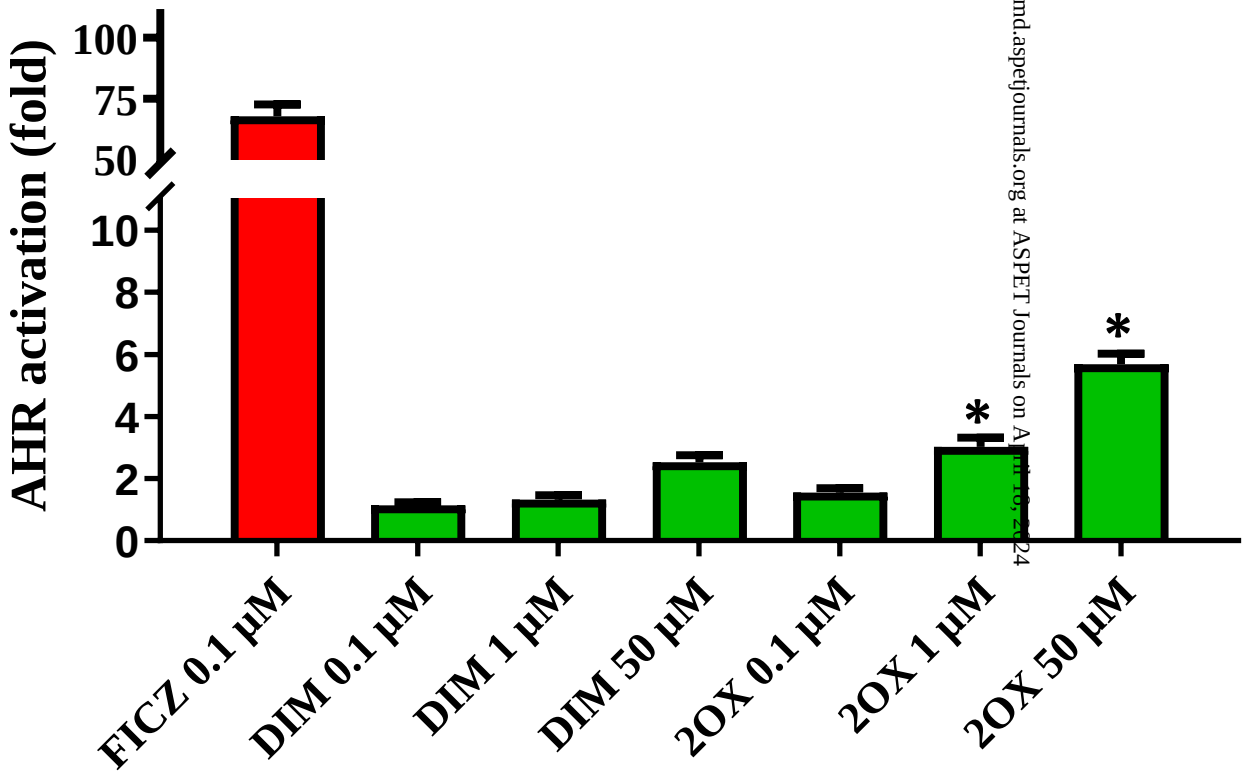




**Figure 8**

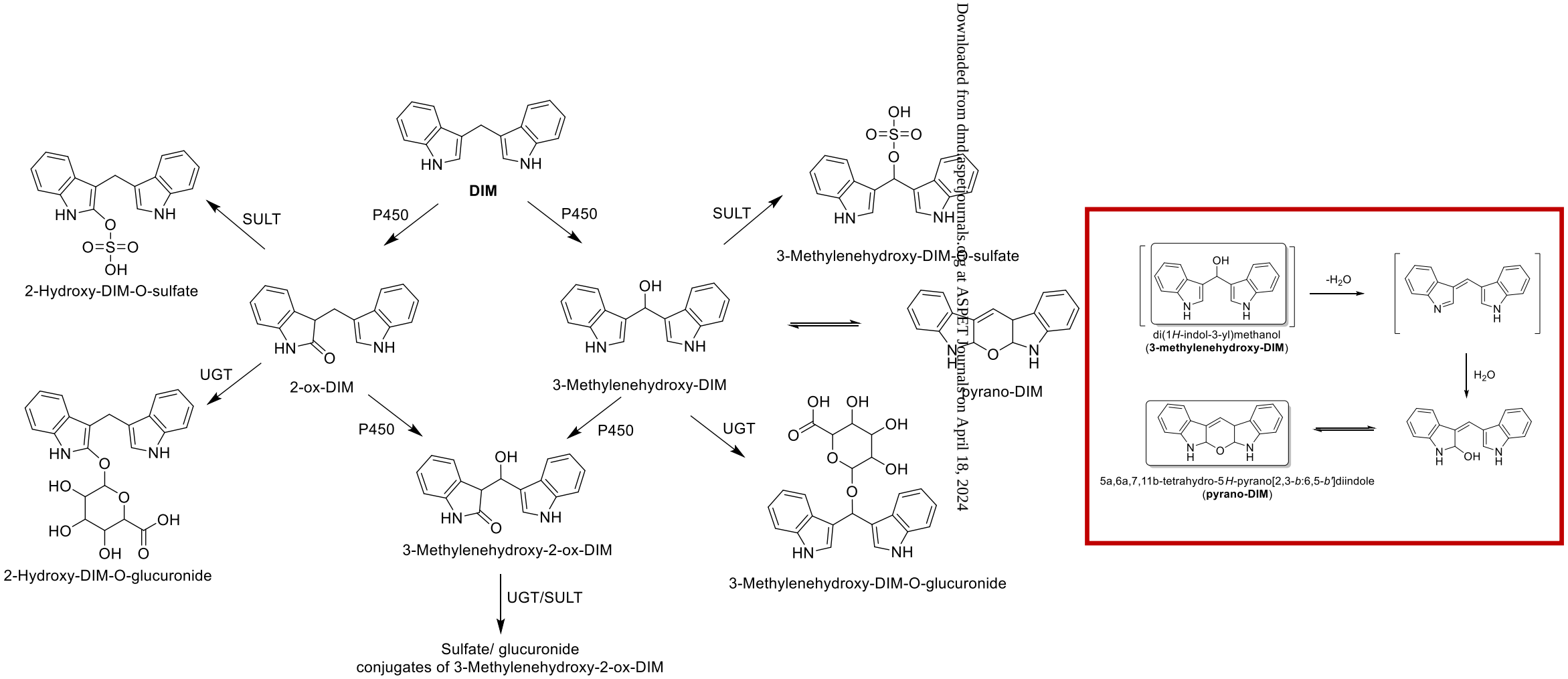




**Figure 9**